

Airborne Pollutants and Lung Surfactant: Biophysical Impacts of Surface Oxidation Reactions

Sahana L. Selladurai

A Thesis

in

The Department

of

Chemistry and Biochemistry

Presented in Partial Fulfillment of the Requirements

for the Degree of Master of Science (Chemistry) at

Concordia University

Montréal, Québec, Canada

September 2015

© Sahana L. Selladurai, 2015

**CONCORDIA UNIVERSITY**

**School of Graduate Studies**

This is to certify that the thesis prepared

By: Sahana L. Selladurai

Entitled: Airborne Pollutants and Lung Surfactant: Biophysical Impacts of Surface Oxidation Reactions

and submitted in partial fulfillment of the requirements for the degree of

**Master of Science (Chemistry)**

complies with the regulations of the University and meets the accepted standards with respect to originality and quality.

Signed by the final examining committee:

\_\_\_\_\_ Dr. Pat Forgione - Chair  
\_\_\_\_\_ Dr. Yves Gélinas - Examiner  
\_\_\_\_\_ Dr. Peter Pawelek - Examiner  
\_\_\_\_\_ Dr. Christine DeWolf - Supervisor

Approved by

\_\_\_\_\_  
Chair of Department or Graduate Program Director

September 2015

\_\_\_\_\_  
Dean of Faculty

## ABSTRACT

### Airborne Pollutants and Lung Surfactant: Biophysical Impacts of Surface Oxidation Reactions

Sahana L. Selladurai

Lung surfactant comprises a lipid-protein film that coats the alveolar surface and serves to prevent alveolar collapse upon repeated breathing cycles. Exposure of lung surfactant to high concentrations of airborne pollutants, for example tropospheric ozone, can chemically modify the lipid and protein components. These chemical changes can impact the film functionality by decreasing the film's collapse pressure (minimum surface tension attainable), altering its mechanical and flow (rheology) properties and modifying lipid reservoir formation essential for re-spreading of the film during the inhalation process. In this research, we use Langmuir monolayers spread at the air-water interface as model membranes where the compression and expansion of the film mimics the breathing cycle. The impact of ozone exposure on model lung surfactant films is measured using a Langmuir film balance, Brewster angle microscopy and a pendant drop tensiometer as a function of film and subphase composition. Oxidation is shown to lower squeeze-out pressure, sometimes alter line tension (and film morphology) and in some cases visibly reduce the viscoelastic properties of the film when compared to controls. These reductions in functionality of the films are highly dependent on film and subphase composition, where for example, the use of a physiologically relevant buffer makes these films more fluid and sometimes more susceptible to oxidation. These findings can lead to a better understanding on the impact of continuous exposure to high levels of ozone on the mechanical process of breathing, as well as understanding the roles of certain lung surfactant components in this process.

## Acknowledgements

The work outlined in this thesis would not have been possible without the support of my family and friends. I would also like to thank my supervisor and research group who have made my M. Sc. experience both enjoyable and memorable.

## Contributions of Authors

All manuscripts and experiments were prepared and carried out by Sahana L. Selladurai under the supervision of Dr. Christine DeWolf. Dr. Rolf Schmidt also contributed with the experimental set-up and data interpretation.

## Table of Contents

Chapter 1. Introduction & Literature Review .....	1
1.1. Model Lung Surfactant Films .....	1
1.1.1. Function & Composition .....	1
1.1.2. Phospholipid Roles .....	1
1.1.3. Cholesterol Roles .....	3
1.1.4. Protein Roles .....	3
1.1.4.1. SP-A & SP-D .....	3
1.1.4.2. SP-B & SP-C .....	4
1.1.5. The Breathing Cycle .....	4
1.1.6. Mechanical Properties: Rheology .....	5
1.2. Lung Surfactant Replacement Therapies .....	7
1.3. Model Lung Surfactant System Studies .....	8
1.4. Effect of Atmospheric Pollutants on Model Lung Surfactant Films .....	9
1.4.1. Environmental Tobacco Smoke .....	9
1.4.2. Particulate Matter .....	9
1.4.3. Tropospheric Ozone .....	9
1.5. Research Objectives .....	13
Chapter 2. Influence of Subphase Composition on Model Lung Surfactant Films .....	16
2.1. Abstract .....	16
2.2. Introduction .....	17
2.3. Materials & Methods .....	18
2.4. Results & Discussion .....	21
2.5. Conclusion .....	32
Chapter 3. Biophysical Impacts of Ozone Exposure on Model Lung Surfactant Films .....	34
3.1. Abstract .....	34
3.2. Introduction .....	34
3.3. Materials & Methods .....	36
3.4. Results & Discussion .....	37
3.5. Conclusion .....	46
Chapter 4. Conclusions and Future Work .....	48

Chapter 5. References ..... 52

## Abbreviations

AFM:	atomic force microscopy
BAM:	Brewster angle microscopy
C:	condensed
DPPC:	dipalmitoylphosphatidylcholine
ESI:	electro-spray ionization
ETS:	environmental tobacco smoke
FIDI:	field induced droplet ionization
GIXD:	grazing incidence x-ray diffraction
HO <sub>2</sub> :	hydroperoxyl radical
IDL:	interactive data language
LE:	liquid expanded
LO:	liquid ordered
LS:	lung surfactant
MS:	mass spectrometry
NMR:	nuclear magnetic resonance
NN:	nearest neighbour
NNN:	next nearest neighbour
NO:	nitric oxide
NO <sub>2</sub> :	nitrogen dioxide
NO <sub>x</sub> :	nitrogen oxides
OH:	hydroxyl radical
PA:	palmitic acid
PAHs:	polycyclic aromatic hydrocarbons
PAT:	profile analysis tensiometer
PBS:	phosphate-buffered saline
PC:	phosphatidylcholine
PG:	phosphatidylglycerol
POPG:	1-palmitoyl-2-oleyl-phosphatidylglycerol
Q <sub>xy</sub> :	in-plane diffraction peaks
Q <sub>z</sub> :	out-of-plane diffraction peaks

RDS:	respiratory distress syndrome
SP :	surfactant-associated proteins
SP-A :	surfactant protein A
SP-B :	surfactant protein B
SP-C :	surfactant protein C
SP-D :	surfactant protein D
TBS :	tris-buffered saline
UV:	ultraviolet

## List of Figures and Tables

Figure 1.1. Representative phospholipids of lung surfactant.....	1
Figure 1.2. Schematic compression isotherm. ....	2
Figure 1.3. Schematic diagram depicting the phase changes of the lung surfactant film during the breathing cycle .....	5
Figure 1.4. Schematic of sources and formation of tropospheric ozone .....	10
Figure 1.5. Ozonolysis of 1-palmitoyl-2-oleoyl- <i>sn</i> -glycero-3-phospho-1-glycerol (POPG) via the Criegee mechanism of ozonolysis. ....	11
Figure 1.6. Schematic depicting the increase in surface pressure attributed to the bending of the oxidized chain.....	12
Figure 1.7. Relationship between different model lung surfactant systems. ....	13
Figure 2.1. Visual depiction of the step through method for rheology measurements. ....	20
Figure 2.2. Isotherms of DPPC:POPG, DPPC:POPG:PA, Infasurf and Survanta. ....	22
Figure 2.3. BAM images of DPPC:POPG on water and TBS. ....	23
Figure 2.4. BAM images of DPPC:POPG:PA on water and TBS. ....	24
Figure 2.5. BAM images of Infasurf on water and TBS.....	25
Figure 2.6. BAM images of Survanta on water and TBS. ....	26
Figure 2.7. Dilational rheology of DPPC:POPG on water and TBS. ....	27
Figure 2.8. Dilational rheology of DPPC:POPG:PA on water and TBS.....	28
Figure 2.9. Dilational rheology of Infasurf on water and TBS.....	28
Figure 2.10. Dilational rheology of Survanta on water and TBS. ....	29
Figure 2.11. $Q_{xy}$ and $Q_z$ fit peaks of DPPC:POPG:PA on TBS.....	30
Table 2.1. $Q_{xy}$ and $Q_z$ of DPPC:POPG, DPPC:POPG:PA, Infasurf and Survanta .....	30
Table 2.2. Lattice and chain tilt parameters of DPPC:POPG, DPPC:POPG:PA, Infasurf and Survanta.....	32
Figure 3.1. Isotherms of DPPC:POPG, DPPC:POPG:PA, Infasurf and Survanta before and after ozone exposure. ....	39
Figure 3.2. BAM images of DPPC:POPG before and after ozone exposure.....	40
Figure 3.3. BAM images of DPPC:POPG:PA before and after ozone exposure. ....	41
Figure 3.4. BAM images of Infasurf before and after ozone exposure. ....	41
Figure 3.5. BAM images of Survanta before and after ozone exposure.....	42

Figure 3.6. Dilational rheology of DPPC:POPG before and after ozone exposure.....	43
Figure 3.7. Dilational rheology of DPPC:POPG:PA before and after ozone exposure.....	43
Figure 3.8. Dilational rheology of Infasurf before and after ozone exposure.....	44
Figure 3.9. Dilational rheology of Survanta before and after ozone exposure.....	44

## Chapter 1. Introduction & Literature Review

### 1.1. Model Lung Surfactant Films

#### 1.1.1. Function & Composition

Lung surfactant (LS) is a monolayer film that coats the inner alveolar surface. This monolayer reduces surface tension to prevent alveolar collapse during exhalation and reduces the work necessary for breathing<sup>1-4</sup>. Natural human LS is composed of phospholipids, neutral lipids and surfactant associated proteins. Specifically, it contains 80 - 90 wt% phospholipids (20 - 30 wt% unsaturated phosphatidylglycerol (PG), 70 - 80 wt% saturated phosphatidylcholines (PC)), 3 - 10 wt% neutral lipids such as cholesterol and 5 - 10 wt% surfactant-associated proteins (SP)<sup>2, 5-7</sup>. Often, dipalmitoylphosphatidylcholine (DPPC) and 1-palmitoyl-2-oleoyl-phosphatidylglycerol (POPG) are used to represent the saturated and unsaturated lipid component respectively as these are the major components of their respective classes<sup>3</sup>. The proteins present in LS are SP-A, SP-B, SP-C and SP-D where SP-B and SP-C are the surface active proteins<sup>8-10</sup>. Each component of LS has its own role in the proper functioning of lung surfactant.

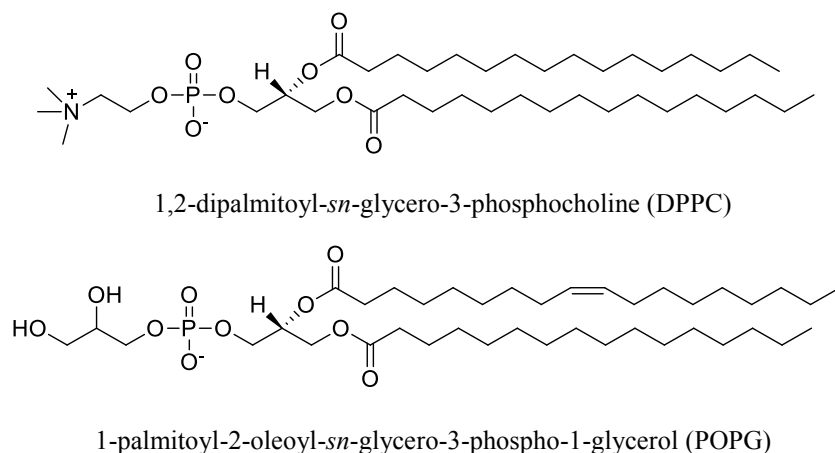


**Figure 1.1. Representative phospholipids of lung surfactant.**

#### 1.1.2. Phospholipid Roles

LS contains both saturated and unsaturated lipids. These two together provide the surface tension reduction capability and the fluidity necessary for re-spreading of the film. In order to better understand the roles of these lipids, it is necessary to understand the phase behaviour of phospholipids. Figure 1.2 shows a schematic compression isotherm of a lipid monolayer at the air-liquid interface. At high molecular area, the lipids are in the gaseous phase where there is little to

no interaction between the lipid molecules and the surface pressure (defined as the difference between the surface tension in the presence and in the absence of a film) remains at zero  $\text{mNm}^{-1}$ . As the monolayer film is compressed, the molecular area is reduced and the lipid molecules interact to form a fluid, liquid expanded (LE) phase where the film has high fluidity and high compressibility. This coherent film reduces the surface tension and so the surface pressure rises as the film is compressed. As the film is compressed even further, some lipids can pack together to form a condensed phase in which the alkyl chains are in their all-trans, fully extended conformation and are closely-packed with liquid-crystalline order. Thus the fluidity and compressibility are lowered. The monolayer collapses when there is no more molecular area available to the lipids. This compression isotherm is a perfect example of the DPPC compression isotherm. With regards to the role of DPPC in lung surfactant, as the film is being compressed, water molecules are being displaced from the air-liquid interface which reduces the surface tension. DPPC efficiently displaces the water molecules since it is able to pack into the condensed phase, allowing it to reach very high surface pressures (low surface tensions, near  $0 \text{ mNm}^{-1}$ ). POPG on the other hand will collapse from the LE phase (at much lower pressures), since the unit of unsaturation does not allow it to pack into a condensed phase. This unsaturation ensures a LE phase is present, and thus provides the fluidity necessary for rapid re-spreading of the film during inhalation.

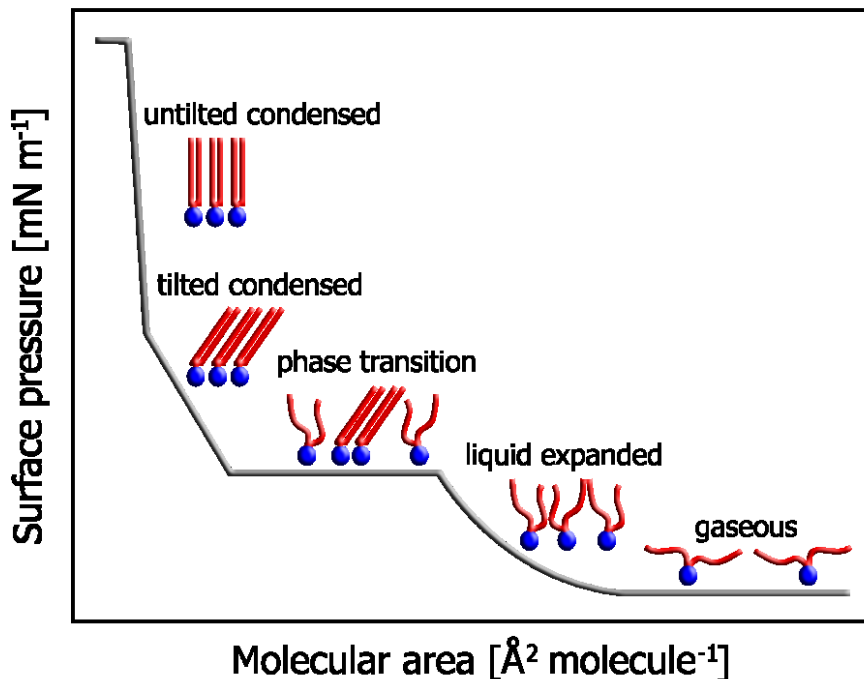


Figure 1.2. Schematic compression isotherm.

### 1.1.3. Cholesterol Roles

Cholesterol is a neutral lipid that is present in native LS. It may affect the structure of the lipid monolayer through intercalation<sup>2</sup>. It plays an important role in lipid phase behaviour and the collapse mechanism, where it is capable of inducing a new phase since domain-in-domain structures (i.e. multiple co-existing phases within a single domain) have been observed in systems with cholesterol<sup>11</sup>. Cholesterol also increases the fluidity and reduces the surface viscosity of model LS films which limits surface tension reduction<sup>12, 13</sup>.

### 1.1.4. Protein Roles

In order to truly understand the breathing cycle, the roles of surfactant-associated proteins must be understood.

#### 1.1.4.1. SP-A & SP-D

SP-A and SP-D are produced by alveolar type II cells<sup>14</sup>. These are glycoproteins with 36 kDa and 43 kDa monomeric polypeptide chains that have been associated with many different roles *in vivo* and *in vitro*<sup>15, 16</sup>. These proteins belong to the collectin family which is mostly known for host defense functions<sup>14, 17</sup>. In the past, however, the functions of these proteins were heavily related to lung surfactant homeostasis. For example, in the case of SP-A, it was found to possibly improve surface adsorption of LS, accelerate monolayer purification, regulate LS lipids by directing them to alveolar type II cells and prevent inactivation of LS by proteins found in blood such as fibrinogen and albumin<sup>15, 18-20</sup>. SP-D was also linked to lipid homeostasis, where mice with targeted SP-D gene mutations were found to accumulate LS lipids with altered lipid structure compared to the wild-type<sup>17</sup>.

More recent research is more focused on the possible immunological roles of SP-A and SP-D. In animal models, a lack of SP-D resulted in no change in bacterial killing compared to the wild-type but without SP-A and SP-D, lung inflammation was more severe<sup>14</sup>. In the case of a viral infection, SP-A and SP-D both inhibited hemagglutination by the virus where SP-D was more effective than SP-A. Also, incubation of the virus with SP-D reduced neutrophil dysfunction enabled by the virus<sup>21</sup>. Furthermore, these proteins have been implicated in stimulating immunological cells when dealing with allergies<sup>22, 23</sup>. Nonetheless, these proteins are not surface-active and therefore will not be explored any further in this thesis research.

#### 1.1.4.2. SP-B & SP-C

On the other hand, SP-B and SP-C are surface-active. SP-B is a 79 amino acid containing 18 kDa homodimer and SP-C is a 35 amino acid peptide with a molecular weight of 4.2 kDa that are released from alveolar type II cells<sup>8, 24-26</sup>. SP-B is a net cationic protein which allows it to interact with anionic lipids such as POPG<sup>25</sup>. Through this interaction, SP-B prevents the loss of material to the subphase since the main function of SP-B is to stabilize the PG molecules squeezed-out from the monolayer near the surface (membrane-membrane associations)<sup>3, 7</sup>. Through solid-state nuclear magnetic resonance (NMR) studies, it was reported that the N-terminal residues of SP-B (insertion sequence) disrupts the ordering within the lipid bilayer (after monolayer collapse). This may provide evidence of SP-B mediating transfer of lipids from the underlying multilayers and the surface<sup>10</sup>. Also, SP-B appears to improve the re-spreadability of the film, where fluorescence images comparing systems with high levels and very low levels of SP-B show that without SP-B the lipid film cracks instead of folding<sup>7</sup>. To add to this, compression-expansion cycles of systems either without SP-B and SP-C or with SP-B or SP-C show that the presence of either protein improves the retention of the lipids thereby greatly improving the reversibility of multilayer formation<sup>27, 28</sup>. Finally, SP-B is an essential protein whereby deficiency is fatal<sup>29</sup>.

Less is known about the role of SP-C, although its main role is thought to be able to retain a continuous fluid phase of the unsaturated lipid, i.e. reservoir formation<sup>7</sup>. This has been evidenced by atomic force microscopy (AFM) images of a lipid-only system supplemented with SP-C showing an increase in film thickness associated with lipid reservoir formation<sup>30</sup>. Also, as mentioned, SP-C improves the reversibility of multilayer formation<sup>27, 28</sup>. SP-C does have two palmitoylated N-terminal cysteine residues<sup>26, 31</sup>. This may be the mechanism involved in reservoir formation<sup>7</sup>.

#### 1.1.5. The Breathing Cycle

The main function of LS as a whole is to enable the breathing process. Figure 1.3 depicts the breathing cycle, where, as we exhale, our LS film is being compressed and as we inhale, our LS film expands. In this figure, exhalation or compression goes downward (steps 1 to 4) and inhalation is upward (steps 4 to 1). Therefore, this entire process is both fast and highly reversible. Initially upon compression (so as we exhale), there is phase separation between the saturated and unsaturated lipid components (step 2). As the film is compressed further there is squeeze-out of

the surfactant proteins and the unsaturated lipid (step 3). Once the proteins and most of the unsaturated lipid are effectively squeezed out, there is reservoir formation (step 4). If there were no surfactant associated proteins, the unsaturated lipids would be lost in the subphase and would take a much longer time to get reincorporated back into the film, which means the reverse of this process, inhalation, would take longer than necessary.

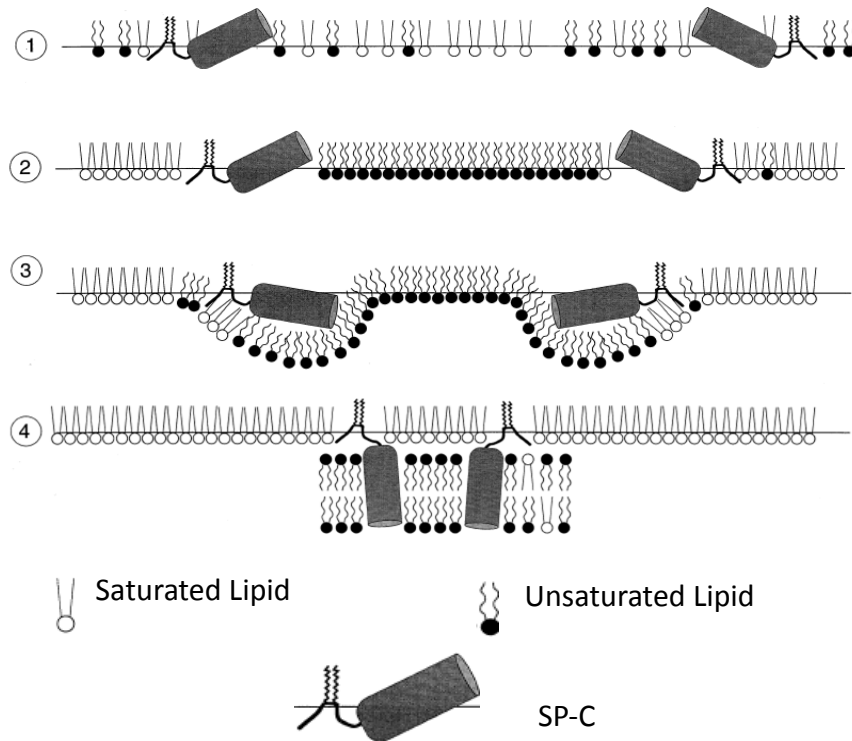


**Figure 1.3. Schematic diagram depicting the phase changes of the lung surfactant film during the breathing cycle <sup>25</sup>.**

#### 1.1.6. Mechanical Properties: Rheology

Rheology or viscoelasticity is defined in terms of elasticity and viscosity. Elasticity is the material's ability to recover after a force is removed and viscosity is the material's resistance to flow after a force is applied. The rheology of monolayers governs the film's stability, function and dynamics <sup>32</sup>. These rheological properties influence the breathing cycle since the LS film must resist the strong deformations associated with the expansion and compression of the lung <sup>33-35</sup>. Specifically dilational rheology is important for the breathing cycle, since this relates oscillations due to changes in surface area and surface tension (or surface pressure) to viscoelasticities <sup>35</sup>.

Like other mechanical properties involved in breathing, LS composition does affect its viscoelastic properties, for example, differing lipid and protein compositions and concentrations result in changes in viscoelasticity<sup>13</sup>. Mixed DPPC and SP-C films exhibited higher surface viscosities than single component films which may support the breathing cycle<sup>35</sup>. Also, addition and supplementation of SP-C or SP-B have been shown to increase the surface shear viscosity of model LS systems<sup>30</sup>. Generally, viscoelastic properties increase with surface pressure<sup>4,36</sup>. Since, during exhalation the surface tension in the alveoli is reduced to near zero and the surface tension in the upper airways stays at 30 mNm<sup>-1</sup>, due to this surface tension gradient, LS should flow out of the alveoli<sup>30</sup>. Therefore, to prevent this outward flow of LS, with increasing alveolar surface pressure (or decreasing surface tension), an increase in surface viscosity should help stabilize LS within the alveoli. The condensed lipid phase found in LS allows collapse to occur at high surface pressure with a high surface viscosity due to a jamming process of the condensed phase domains. Therefore, a LS film should at high surface pressure, have high surface viscosities and at low surface pressure have low surface viscosities to maximize the collapse pressure during compression and to facilitate re-spreading of the surfactant film during expansion<sup>4</sup>.

## 1.2. Lung Surfactant Replacement Therapies

Lung surfactant replacement therapies are used to treat respiratory distress syndrome (RDS) in pre-term babies <sup>37</sup>. These therapies are typically derived from bovine or porcine lung lavages. Where, the surface-inactive proteins such as SP-A and SP-D are removed. There are a multitude of lung surfactant replacement therapies available. Curosurf, Infasurf and Survanta are commonly used and are compositionally comparable. Curosurf is derived from porcine lung lavages and Infasurf and Survanta are derived from the bovine. All three of these therapies contain similar amounts of phospholipids, however, Survanta contains added free fatty acids (palmitic acid (PA)) and they all contain differing amounts of SP-B. In terms of SP-B, Infasurf contains high amounts, Curosurf contains moderate amounts and Survanta contains low amounts. In the case of SP-C, Survanta, Infasurf and Curosurf contain moderate amounts <sup>11,38</sup>. Based on the compositional differences, clinical performance can be evaluated.

When comparing Survanta and Curosurf, Curosurf performed better clinically when treating RDS. Specifically, infants treated with Curosurf as opposed to Survanta had a reduced need for more than one dosing, a reduced need for supplemental oxygen and a reduced mortality rate <sup>39</sup>. However, when comparing clinical trials using Survanta versus Infasurf, the biggest difference was that the dosing intervals were longer for Infasurf than Survanta <sup>40</sup>. This means that Infasurf has a longer lasting effect. On a surface activity standpoint, Survanta has lower adsorption and surface tension reducing ability than Infasurf. The authors correlate the poor performance of Survanta to reduced levels of SP-B, since supplementing Survanta with SP-B improved the surface activity to be comparable to Infasurf <sup>9</sup>. Understanding the role of composition in the performance of lung surfactant replacement therapies can lead to optimization of such treatments in the future. Lung surfactant replacement therapies can be used as model LS systems to study differences in biophysical properties induced by compositional changes.

### 1.3. Model Lung Surfactant System Studies

Multiple methods are used to study the biophysical properties of model LS films as outlined throughout this literature survey. These methods include: atomic force microscopy (AFM), compression isotherms, isotherm cycling, Brewster angle microscopy (BAM), fluorescence imaging and grazing incidence x-ray diffraction (GIXD) among others. AFM consists of depositing films on a solid substrate to visualize reservoir formation through analysing changes in film thickness <sup>30</sup>. Compression isotherms allow us to establish changes in surface activity, for example, a reduction in surface activity is shown by a decrease in collapse surface pressure and therefore a lower surface tension reduction ability of the film <sup>9</sup>. Further, isotherm cycling (compression-expansion cycles) is used to determine the recovery of the film following squeeze-out of the LE phase where shifts of the isotherm to lower molecular area means a loss of material from the interface <sup>27, 28</sup>. Upon compression and expansion, BAM and fluorescence imaging are used to determine changes in morphology (domain size and shape) <sup>7</sup>. Finally, GIXD measurements provide information about the ordering and structure of the film, where structural changes may be induced based on differences in film composition <sup>4, 41, 42</sup>. These techniques can be used to establish changes in the biophysical properties of model LS films induced by exposure to atmospheric pollutants.

## 1.4. Effect of Atmospheric Pollutants on Model Lung Surfactant Films

Atmospheric pollutants are a result of anthropogenic and biogenic sources. This review will focus on the effect of environmental tobacco smoke, particulate matter or nanoparticles and ozone on the biophysical properties of model LS films.

### 1.4.1. Environmental Tobacco Smoke

Environmental tobacco smoke (ETS) is second-hand smoke. A recent study found that exposing Survanta and Curosurf monolayers to ETS-exposed water led to reduced biophysical properties of the monolayer<sup>43</sup>. Compression isotherms showed a reduction in the collapse pressure of the film leading to a lowering of the film's surface tension reduction ability. AFM images showed a reduction in film thickness correlating to a decrease in lipid reservoir retention. These reductions may be due to oxidation of the films since Survanta was affected less than Curosurf. Curosurf does contain more SP-B and unsaturated phospholipids than Survanta<sup>11</sup>.

### 1.4.2. Particulate Matter

Fine (< 250 nm) and ultrafine (< 100 nm) particulate matter or nanoparticles can penetrate into the lower airways and come into contact with LS<sup>44</sup>. Nanoparticles have been shown to be able to interact with the lipids in the monolayer and change the properties of the film<sup>44-47</sup>. Exposing gold nanoparticles to model LS films reduced the film's surface activity, its ability to re-spread upon expansion, and the PG lipids coated the nanoparticle surface<sup>44</sup>. DPPC has also been shown to coat the surface of citrate-capped silver nanoparticles<sup>45</sup>. These lipid-nanoparticle interactions can change the lipids' phase behaviour and therefore its role within the breathing cycle. Silica nanoparticles do modify monolayer phase behaviour due to formation of lipid-nanoparticle complexes. This ultimately reduced the viscoelasticity of the film<sup>46,47</sup>.

### 1.4.3. Tropospheric Ozone

Tropospheric ozone or ground-level ozone is mainly a result of a series of reactions concerning other atmospheric pollutants. A simplified reaction scheme for production of tropospheric ozone (Fig. 1.4) begins with hydroxyl radicals (OH) reacting with hydrocarbons and oxygen to give carbon dioxide, water and hydroperoxyl radicals (HO<sub>2</sub>). The HO<sub>2</sub> produced in the first reaction set then reacts with nitric oxide (NO) to form more OH and nitrogen dioxide (NO<sub>2</sub>),

where finally  $\text{NO}_2$  reacts with oxygen and ultra-violet (UV) radiation to give more NO and tropospheric ozone<sup>48-50</sup>. NO and hydrocarbons are the main sources of tropospheric ozone. These pollutants come from sources such as fossil-fuel burning, biomass burning, vegetation, wetlands, animal waste, landfills and others<sup>49</sup>. Currently, average ground-level ozone concentrations range from approximately 30 to 40 ppb, whereas the pre-industrial era averaged a concentration of approximately 10 to 15 ppb. This increase in ozone concentration has been linked to an increase in nitrogen oxide ( $\text{NO}_x$ ) emissions resulting from fossil fuel burning<sup>48, 51</sup>. A less significant source of tropospheric ozone comes from the stratosphere as gases are constantly exchanged between the troposphere and the stratosphere<sup>52</sup>.

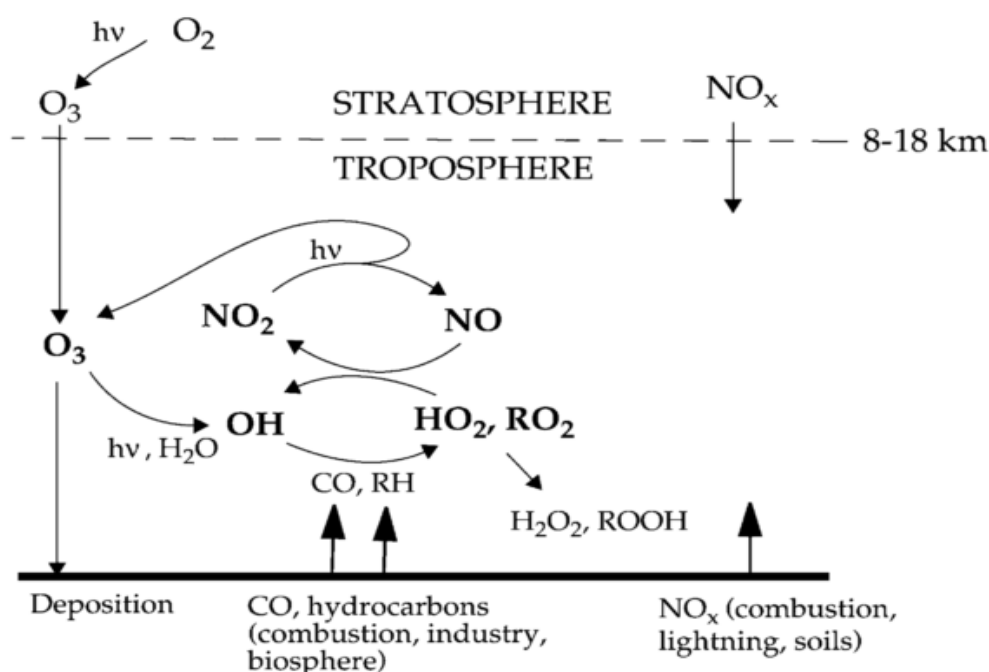


**Figure 1.4. Schematic of sources and formation of tropospheric ozone<sup>50</sup>.**

Ozone is capable of absorbing infrared radiation and is therefore a greenhouse gas<sup>48, 50, 53</sup>. High concentrations of ozone can contribute to global warming and affect the climate but it may also affect human health. Incidences where high ozone concentrations have been reported are during photochemical smog, where ozone concentrations can be over 220 ppb<sup>48, 54</sup>. Significant research has gone into studying the effect of inhaling high ozone concentrations on pulmonary function and exacerbations or onset of respiratory diseases such as asthma. For example, exposing asthmatic adult males to only 200 ppb ozone for 6 hours alternating rest and exercise periods led to increases in inflammatory markers within their airways which were not apparent in non-

asthmatic males. Yet, this ozone concentration did not appear to reduce lung function<sup>55</sup>. However, in other studies that correlated lifetime ozone exposures in adult males to lung function found a negative effect which was associated with decreased airway function<sup>56,57</sup>. In another correlation study, which was relating mortality from respiratory illnesses and ozone concentration, found that death from respiratory causes increased with increasing ozone concentrations. Specifically, with every 10 ppb increase, there was an approximate 3 % increase in deaths associated with respiratory illnesses<sup>58</sup>. Further, when using mice models, exposure of 1 ppm ozone over the course of 3 hours prompted the clinical symptoms of asthma<sup>59</sup>.

This shows that exposure to ambient to high concentrations of ozone does indeed have an effect on human and animal respiratory health. However, relatively little research has gone into studying the effect of ozone exposure on the mechanical properties of the lung surfactant film, the primary contact between the air and the rest of the pulmonary system.

Interfacial exposure of both unsaturated and saturated phospholipids found in LS to ozone lead to oxidation of the unsaturated lipid but not the saturated lipid. The unsaturated lipid reacts with ozone via the Criegee mechanism of ozonolysis to give aldehyde, carboxylic acid and peroxide reaction products (Fig. 1.5)<sup>60,61</sup>.

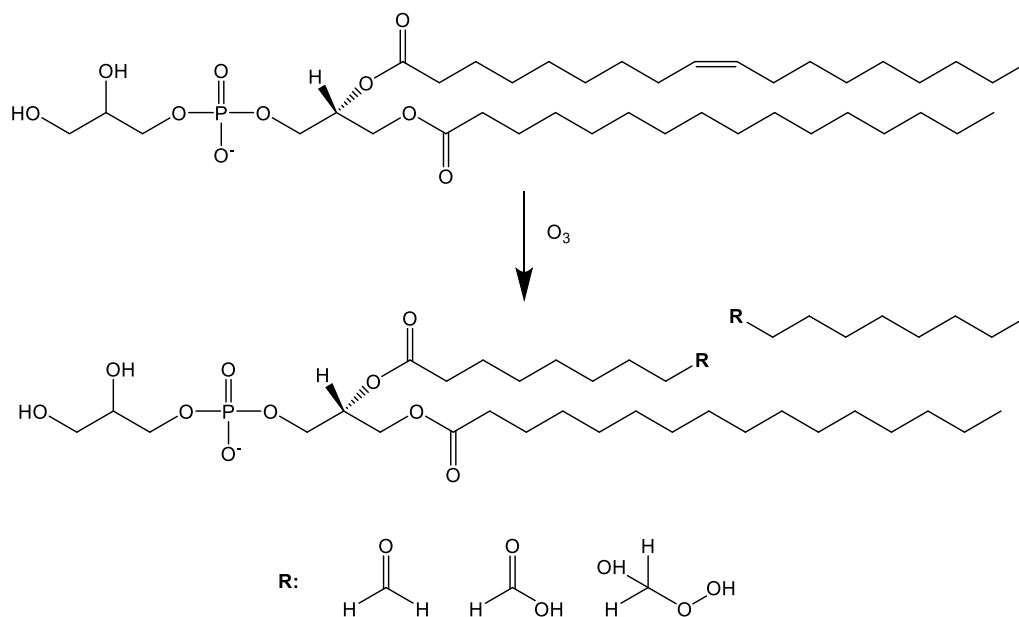


**Figure 1.5. Ozonolysis of 1-palmitoyl-2-oleoyl-*sn*-glycero-3-phospho-1-glycerol (POPG) via the Criegee mechanism of ozonolysis.**

As a result, oxidation of the unsaturated lipid component leads to an increase in surface pressure which may be attributed to the now remaining chain bending to penetrate the air-liquid

interface as depicted in Figure 1.6<sup>62</sup>. A truncated SP-B form has also been shown to be oxidized by ozone, where a triply oxygenated product was observed using field induced droplet ionization mass spectrometry (FIDI-MS)<sup>63</sup>. Further studies in terms of changes in the biophysical properties of model LS films after ozone exposure have been lacking.

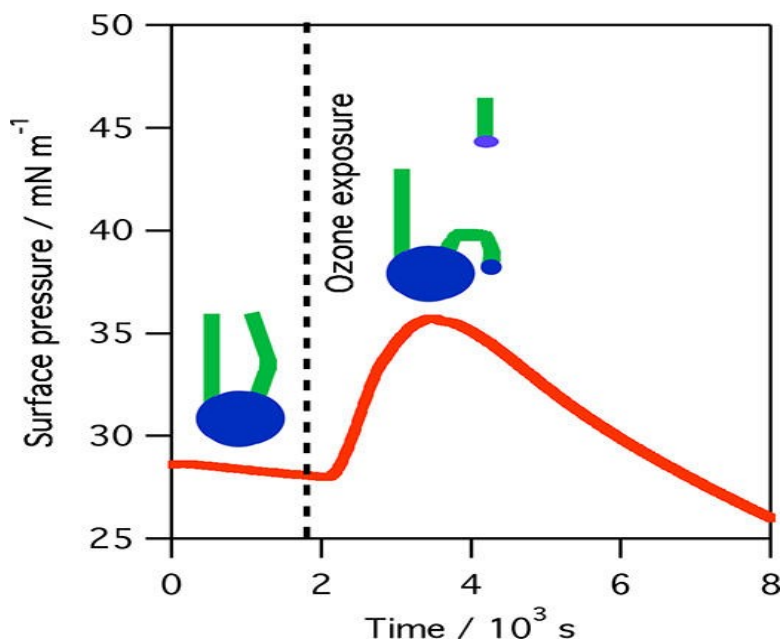


**Figure 1.6.** Schematic depicting the increase in surface pressure attributed to the bending of the oxidized chain<sup>62</sup>.

## 1.5. Research Objectives

Our research focuses on studying the impact of ozone exposure on the surface activity, morphology and rheology of model lung surfactant films as a function of composition. The model lung surfactant films used are a DPPC:POPG mixture, Infasurf, a DPPC:POPG:PA mixture, and Survanta. Using these systems will allow us to understand the effect of composition. Referring to Figure 1.7, DPPC:POPG and Infasurf can be used to study the effect of the addition of surfactant proteins. DPPC:POPG:PA and Survanta can also be compared to study the effect of the addition of proteins. DPPC:POPG and DPPC:POPG:PA can be compared to study the effect of the addition of palmitic acid. Finally, Infasurf and Survanta can be compared to study the effect of differing amounts of SP-B. This approach will allow us to study the effect of lung surfactant composition systematically. To take this work one step further, the effect of using water versus a physiologically relevant buffer was also studied since a salt effect is expected when using these lipids. Moreover, systems studied in the literature vary significantly in subphase composition.

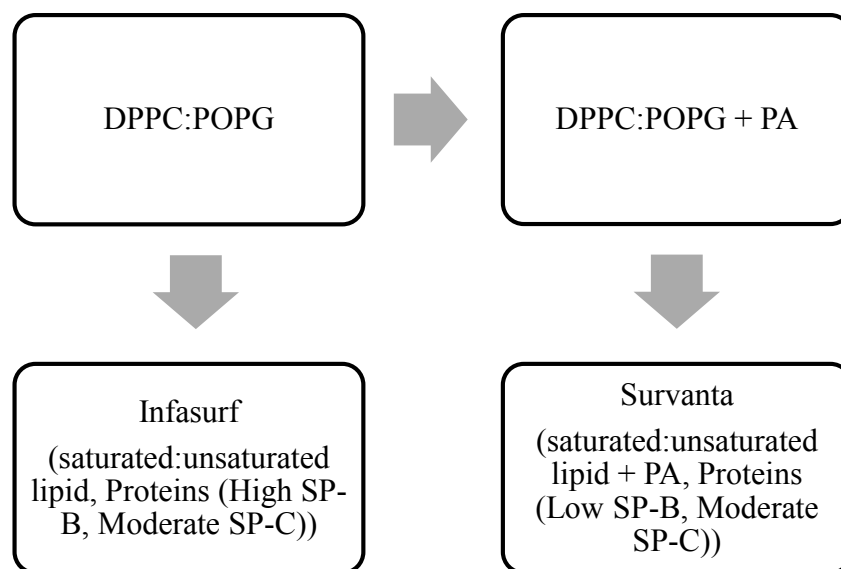


**Figure 1.7. Relationship between different model lung surfactant systems.**

Unsaturated lipids present in these systems, predominantly POPG, can be oxidized by ozone leading to cleavage of the double-bond. This can result in changes to the mechanical properties of the film, since now the oxidized lipids have become more soluble and as shown previously<sup>62</sup> the cleaved chain has an altered conformation at the surface. Also, with the presence of surfactant proteins, oxidizable amino acids such as cysteine, methionine, tryptophan, histidine and phenylalanine are being introduced to the system. Oxidation of these proteins may lead to

changes in their behaviour, for example their interaction with the lipid molecules present in the film. Surface activity and rheological changes were monitored using a profile analysis tensiometer (PAT) and morphological studies were done using a Brewster angle microscope (BAM) with a Langmuir film balance.

Two manuscripts are included in this thesis research (Chapters 2 & 3). The first manuscript (Chapter 2) focuses on studying the surface activity, morphology, rheology and monolayer structure (using grazing incidence x-ray diffraction (GIXD)) of the four systems as a function of subphase. The two subphases used were water and tris-buffered saline (TBS) as a more physiologically-relevant subphase. The study of the influence of subphase on model LS films is important because most of the literature on LS focuses on either water or buffer as the subphase but the comparison between the two is lacking. Therefore, a systematic study of the influence of using water or a physiologically-relevant buffer (tris-buffered saline) subphase on model LS films was carried out using a combination of compression isotherms, Brewster angle microscopy images, rheological data and grazing incidence x-ray diffraction data. The results of these methods will allow us to deduce possible changes in surface activity, morphology, viscoelasticity and monolayer structure due to the presence of salt. Depending on the composition of the film, the salt may have more or less of an impact. However, we generally expect an increase in the fluidity of the film when using a buffer as opposed to water as the subphase since POPG is anionic and consequently we expect a counterion effect.

The final manuscript (Chapter 3) focuses on the impact of ozone exposure on the surface activity, morphology and rheology of all four systems as a function of film composition while using a physiologically-relevant subphase. Lung surfactant is the first point of contact between the lungs and the atmosphere. In areas of high industrial or transportation activity, tropospheric ozone concentrations can be quite high. Therefore, it is important to study the impact of ozone exposure on LS. To do this, we use model LS films such as DPPC:POPG, DPPC:POPG:PA, Infasurf and Survanta to see the effect of exposure based on compositional differences. Changes in LS films' surface activity, morphology and rheology were monitored via profile analysis tensiometer and Brewster angle microscopy. Since POPG can be oxidized due to the presence of the double-bond, changes in the mechanical properties of LS are expected. Further, the data obtained can be used to ameliorate lung surfactant replacement therapies used to treat respiratory ailments and lead to a

better understanding of the impact of pollutants on the breathing cycle. The final chapter of this work (Chapter 4) offers an overall conclusion and directions for the future.

## Chapter 2. Influence of Subphase Composition on Model Lung Surfactant Films

This manuscript has been prepared for submission to Chemistry and Physics of Lipids with the following authorship: Sahana Selladurai, Rolf Schmidt and Christine DeWolf.

### 2.1. Abstract

Lung surfactant replacement therapies, Survanta and Infasurf, and two lipid-only systems both containing saturated and unsaturated phospholipids and one containing additional palmitic acid were used to study the impact of salt in the subphase on the surface activity, morphology, rheology and structure of these monolayers. Changes in surface activity and rheology were measured using a profile analysis tensiometer (PAT), changes in morphology were observed using a Langmuir film balance equipped with a Brewster angle microscope (BAM) and changes in monolayer structure were monitored using grazing incidence x-ray diffraction (GIXD). The lipid-only systems exhibited a film expansion in the presence of salt attributed to more liquid expanded (LE) phase possibly due to intercalation of sodium cations between the negatively charged lipid headgroups. Similarly, the charged palmitic acid headgroups may also have been affected by counterions through such an interaction. Survanta and Infasurf on the other hand displayed more complicated behaviour. The compression isotherms of these two systems do show an expansion of the film; as does the rheology measurements of Survanta, where there is a reduction in viscoelasticity, but not Infasurf. This may be because Infasurf contains high amounts of SP-B which is positively charged so that the effect of salt is minimized. Despite this, the film morphology shows little or no difference with the change of subphase. GIXD measurements indicate that the tilt angles of the DPPC-rich condensed phase of Infasurf exhibits a slight expansion leading to greater tilt angles on buffer. These results highlight that the choice of subphase and use of a physiologically relevant buffer is important for meaningful measurements using model systems.

## 2.2. Introduction

Lung surfactant (LS) coats the inner surface of the lung and serves to reduce surface tension to prevent alveolar collapse during exhalation<sup>1-3</sup>. It also reduces the work necessary for breathing<sup>3,4</sup>. LS is composed of 80 - 90 wt% phospholipids, of which 20 - 30 wt% is unsaturated and 70 - 80 wt% is saturated, it also contains 3 - 10 wt% neutral lipids which are predominately cholesterol and 5 - 10 wt% surfactant-associated proteins<sup>2,5-7</sup>. These proteins include SP-A, SP-B, SP-C and SP-D of which SP-B and SP-C are the surface active proteins that are responsible for membrane-membrane associations and reservoir formation respectively<sup>8-10</sup>. Langmuir monolayers are frequently used as model membranes for lung surfactant systems<sup>7,41</sup>. Dipalmitoylphosphatidylcholine (DPPC) is often used to represent the saturated lipid component and 1-palmitoyl-2-oleoyl-phosphatidylglycerol (POPG) the unsaturated lipid component<sup>3</sup>, although there is a plethora of work using lung surfactant replacement therapies<sup>4,7,9,11</sup> as model systems.

Multiple factors can influence the biophysical properties of these model membranes. This includes composition and spreading conditions of the system but also composition of the subphase, i.e. pH, salt composition and concentration. Although, lung surfactant model systems have been studied extensively throughout the literature, water and buffer have been used interchangeably as the subphase with scarce direct comparisons despite the wealth of data on the impact of salts and counterions on lipid monolayers<sup>64-70</sup>.

The focus of this work is a study of the impact of a buffered subphase on both lipid only and lipid-protein lung surfactant models; the choice of subphase is important in order to understand the behaviour of these films under physiological conditions. The physiologically relevant buffer used in this study is tris-buffered saline (TBS), where the salt content is exclusively sodium chloride. Sodium and potassium cations are the most abundant in intracellular and extracellular fluids<sup>67,71</sup>, sodium cations have been shown to have a more significant impact on lipid membranes than potassium cations<sup>68</sup>. Moreover, monovalent cations are more important in the context of lipid membranes<sup>68</sup> while divalent cations are more important in the context of mitochondrial membranes. The impact of the counterion is highly dependent on the composition of the monolayer film, namely the relative amounts of charged and uncharged lipids and the presence or absence of surfactant proteins, which themselves may act as highly localized counterions. Four model systems were selected and include: DPPC:POPG, DPPC:POPG:PA, Infasurf and Survanta. These systems

were chosen based on composition, where Infasurf and Survanta are lung surfactant replacement therapies and can be used to study the effect of the presence of protein. Both of these therapies contain saturated and unsaturated phospholipids as well as SP-B and SP-C, but, Infasurf contains approximately 0.9 %w/w SP-B and 0.7-1.3 %w/w SP-C whereas Survanta contains approximately 0.04 %w/w SP-B and 0.9 %w/w SP-C<sup>11</sup>. Survanta also contains added palmitic acid. DPPC:POPG:PA mixtures are often used as a mimetic of this system. DPPC:POPG monolayers have been studied thoroughly on water, but less so on buffer<sup>41</sup>. On the other hand, DPPC:POPG:PA and Survanta systems have been studied on both water and buffer, but with different spreading conditions, i.e. DPPC:POPG:PA spread from chloroform and Survanta from a diluted aqueous suspension<sup>3, 6, 41</sup>. Like Survanta, Infasurf is also usually spread from an aqueous suspension but there is a lack of data on both buffer and water<sup>6</sup>. The compositional variations in these four systems will allow us to discern the roles of different membrane components in lung surfactant functioning and the extent to which they are affected by subphase counterions.

### 2.3. Materials & Methods

**Materials.** Dipalmitoylphosphatidylcholine (DPPC, > 99 %) and 1-palmitoyl-2-oleoyl-phosphatidylglycerol (POPG, > 99 %) were purchased from Avanti Polar Lipids. Palmitic acid (PA, > 99 %), tris(hydroxymethyl)aminomethane (tris, > 99.8 %), NaCl salt (> 99 %) and phosphate-buffered saline tablets (PBS, pH 7.4, 10 mM phosphate, 137 mM NaCl, 2.7 mM KCl) were all purchased from Sigma-Aldrich. Survanta and Infasurf are lung surfactant replacement therapies that were donated by Abbott Laboratories and Ony Inc. respectively. The spreading solvent used in all experiments conducted was HPLC grade chloroform obtained from Fisher Scientific.

**Preparation of Mixtures, Solutions & Subphases.** The DPPC:POPG and the DPPC:POPG:PA mixtures were prepared using stock solutions of DPPC, POPG, and PA to achieve molar ratios of 77:23 and 61:19:20 respectively, all of which were prepared in chloroform. The Infasurf and Survanta solutions were prepared by introducing weighed lyophilized sample into chloroform. Water subphases comprised of Ultrapure water with a resistivity of 18.2 M $\Omega$  cm<sup>-1</sup> from a Barnstead Easypure II LF purification system. The tris-buffered saline (TBS) was prepared by using 50 mM tris and 150 mM NaCl in ultrapure water, where the pH was adjusted to

7.4 using hydrochloric acid and the phosphate-buffered saline (PBS) was prepared by dissolving one PBS tablet in 200 mL ultrapure water.

**Surface Activity and Rheology.** Surface activity and rheological measurements were carried out using a SINTERFACE Technologies profile analysis tensiometer (PAT), where a model lung surfactant monolayer solution in chloroform with a concentration of less than 0.1 mg mL<sup>-1</sup> was spread on a 10  $\mu$ L drop of subphase. The spreading volume ranged from 0.4 to 0.8  $\mu$ L. After spreading, the surface area of the pendant drop was expanded from 25 to 40 mm<sup>2</sup>. The drop was then left to equilibrate for an additional 3 minutes to allow for complete evaporation of the chloroform and possible rearrangement of the membrane components. For surface activity measurements, surface pressure-area isotherms were obtained using a molecular compression speed of 0.06 mm<sup>2</sup>s<sup>-1</sup>. Rheological measurements were done by using a step through method (Fig. 2.1). From the initial surface area of 40 mm<sup>2</sup> the film is compressed to 26.8 mm<sup>2</sup> at a compression speed of 0.06 mm<sup>2</sup>s<sup>-1</sup>, the drop was then left to equilibrate for 300 s after which the drop volume was oscillated for 600 s with an amplitude of 0.5 mm<sup>2</sup>, and a frequency of 0.01 s<sup>-1</sup> (100 s period, 6 oscillations). The drop was then left to equilibrate for 180 s, before compressing to the next surface area, equilibrated (300 s) and oscillated once again using the same parameters. This cycle was continued until a surface tension of around 25 mNm<sup>-1</sup> was reached, giving rheological data for surface pressures ranging from 10 to 45 mNm<sup>-1</sup>. This rheological data yields the dilational surface elasticity and viscosity of the monolayer <sup>72</sup>.

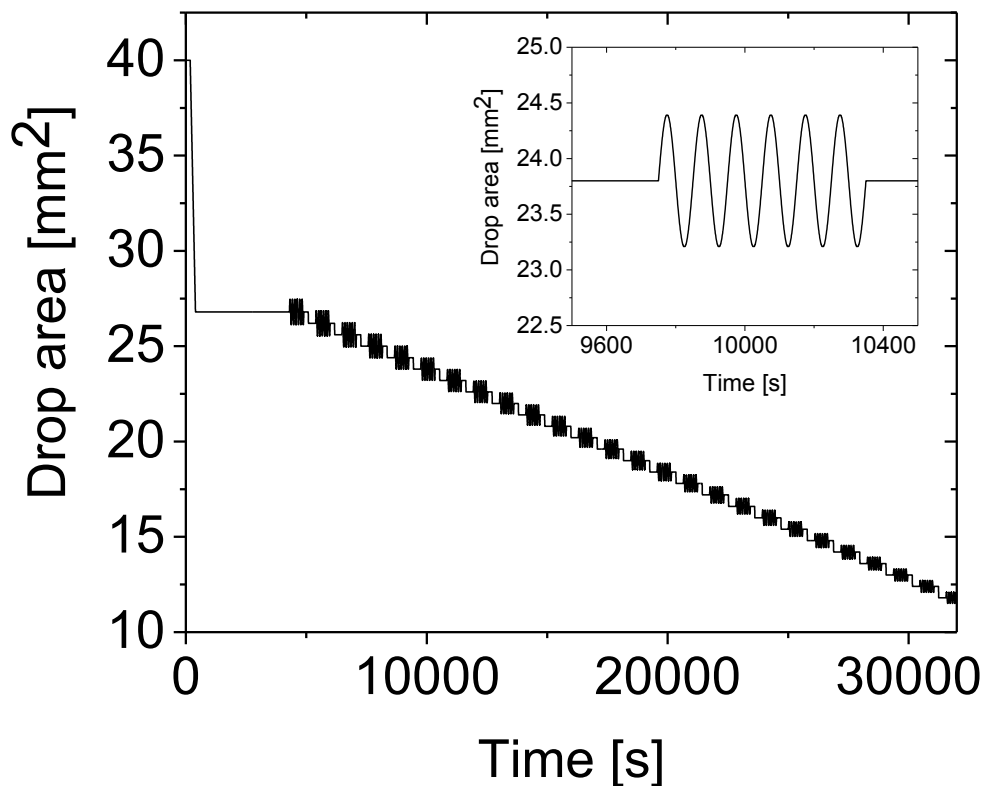


**Figure 2.1.** Visual depiction of the step through method for rheology measurements.

**Brewster Angle Microscopy.** Brewster angle microscopy (BAM) was performed on films spread from a concentration of less than  $1.0 \text{ mg mL}^{-1}$  in chloroform on a Langmuir film balance (NIMA technology) coupled with an I-Elli2000 imaging ellipsometer (I-Elli2000, Nanofilm Technologies). This instrument is equipped with a 50 mW Nd:YAG laser ( $\lambda = 532 \text{ nm}$ ) and images were obtained using a 20X magnification lens with a lateral resolution of  $1 \text{ }\mu\text{m}$  and a  $53.15^\circ$  incident angle. For these films, a compression speed of  $5 \text{ cm}^2 \text{ min}^{-1}$  was used.

**Grazing Incident X-Ray Diffraction.** Grazing incident x-ray diffraction (GIXD) measurements were done at the Advanced Photon Source at Argonne National Laboratories at the ChemMatCARS 15-ID-C beamline. The x-ray beam wavelength, incident angle, horizontal size and vertical size were  $1.239 \text{ \AA}$ ,  $0.0906^\circ$ ,  $20 \text{ }\mu\text{m}$  and  $120 \text{ }\mu\text{m}$  respectively. These parameters led to a beam footprint of  $20 \text{ }\mu\text{m} \times 7.6 \text{ cm}$ . A two-dimensional Swiss Light Source PILATUS 100 K detector was used in single-photon counting mode. In order to minimize intense low-angle scattering, two sets of slits were used. One was placed  $292.0 \text{ nm}$  from the sample and the other was placed in front of the detector. Measurements were taken at the air-liquid interface of a  $340 \text{ cm}^2$  Langmuir-Blodgett trough after spreading solutions similar to the ones used for BAM. Data

was then analyzed using Interactive Data Language (IDL) and Origin. The in-plane diffraction peaks ( $Q_{xy}$ ) and the out-of-plane diffraction peaks ( $Q_z$ ) were fit with Lorentzian and Gaussian functions respectively. These measurements provide information about the ordering and structure of the film.

## 2.4. Results & Discussion

The two lipid-only systems were studied using PBS and TBS. Both subphases provided very similar compression isotherms (Appendix A, Fig. A1 & A2), however, significant line tension differences were observed in the domain morphology with the addition of palmitic acid when the subphase comprised of PBS. For this reason, TBS was used to study the impact of buffer on model lung surfactant films.

The compression isotherms of all four lipid and lipid-protein systems on water and TBS are shown in Figure 2.2. In all cases, a shift to higher molecular areas can be observed when using a buffered subphase. DPPC is zwitterionic and is known to form a condensed phase at pressures above  $8 \text{ mNm}^{-1}$ <sup>32</sup> while POPG is anionic, and forms a liquid-expanded (LE) phase at all pressures above  $0 \text{ mNm}^{-1}$ <sup>30</sup>. In the case of the DPPC:POPG mixture, the buffer has no impact when both components are in the LE phase. However, above the LE-condensed (C) phase transition, there is a shift to higher molecular areas for the buffered system (or conversely, an increase in the surface pressure at a given area) in agreement with the literature on the effects of salt on DPPC<sup>69</sup>. The expansion of the film can also be attributed to the penetration of sodium cations into the headgroup region of the POPG molecules, which allows for intercalation of the cations between the anionic headgroups of the lipids<sup>66</sup>. For the DPPC:POPG:PA system, these shifts are evident at both lower and higher pressures. Also, the phase transition plateau becomes more apparent and higher in surface pressure. The presence of palmitic acid normally increases the collapse pressure since the single saturated hydrocarbon chain makes PA highly compressible. The addition of salt should also increase the collapse pressure when PA is present since the sodium cations are free to bind to the deprotonated carboxylic headgroups of PA exhibiting a counterion effect which is also possible with POPG<sup>70</sup>. However, this is difficult to see in our compression isotherms since the attainable surface pressures were not high enough (Fig. 2.2). Interpretation of the salt effects on Infasurf and Survanta systems are more complicated due to the complexity of the composition (two charged proteins and more complex lipid composition). In both of the systems, it is evident that the film is

more expanded on TBS than on water, and the squeeze-out pressures are lower when salt is present. This could be due to the presence of surfactant proteins as well as other lipids found in these systems.

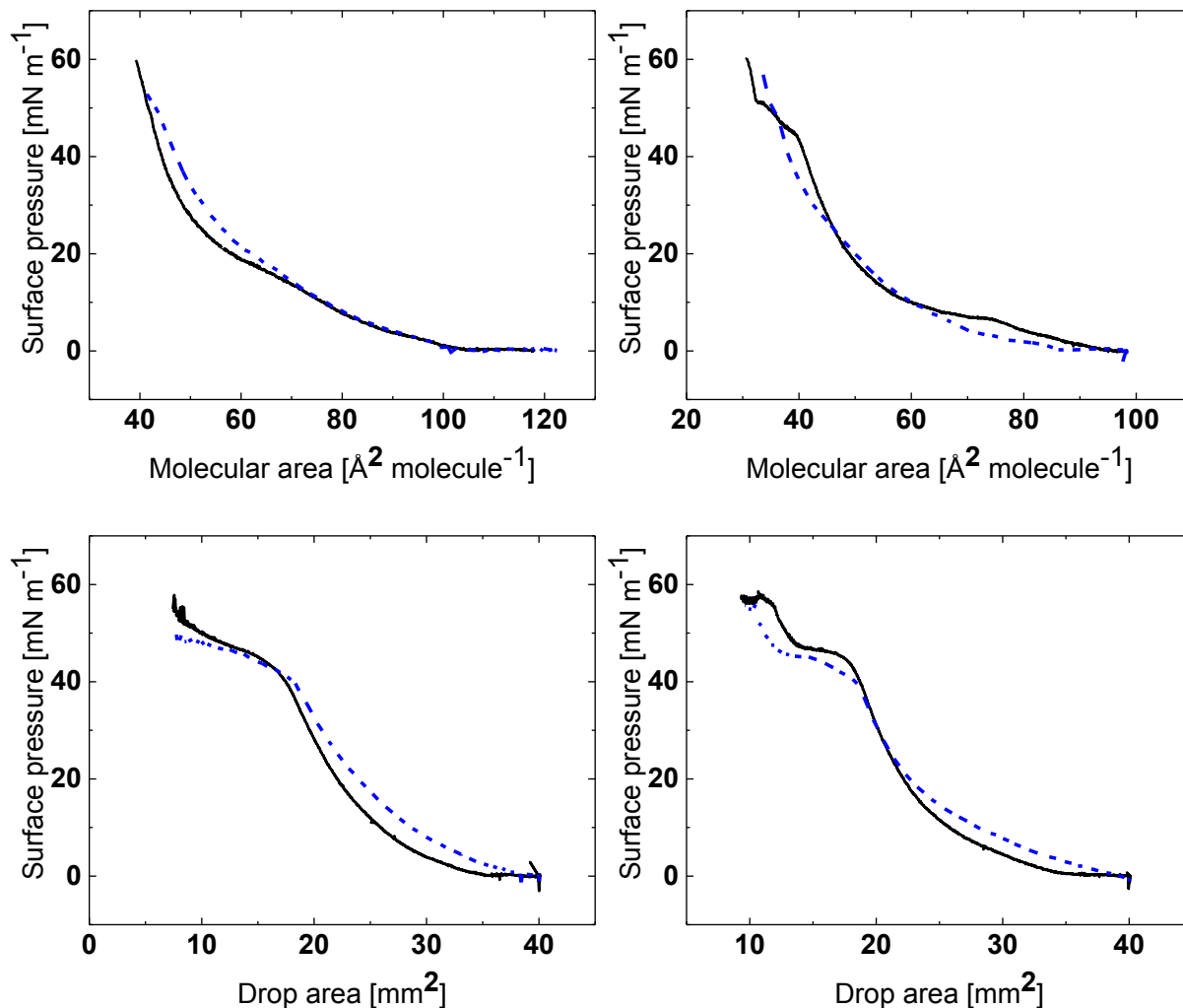


**Figure 2.2.** Isotherms of DPPC:POPG (top, left) , DPPC:POPG:PA (top, right), Infasurf (bottom, left) and Survanta (bottom, right) monolayers on water (—) and TBS (---) at 23 °C. Note that the isotherms of the lipid-protein systems are plotted as a function of drop area as the average molecular weight is unknown for natural extracts.

BAM images of all four systems are shown in Figures 2.3 to 2.6. The images for DPPC:POPG show that at pressures above  $20 \text{ mNm}^{-1}$ , there is significantly more LE phase on TBS than on water which correlates with the expansion observed in the compression isotherm. The squeeze-out of the LE phase occurs earlier on water than on buffer (although this is more difficult to distinguish in PAT isotherms compared to classical Langmuir film balance isotherms <sup>73</sup>) which may be because of the counterion effect on POPG which stabilizes the charge repulsion present in the monolayer at higher pressures.

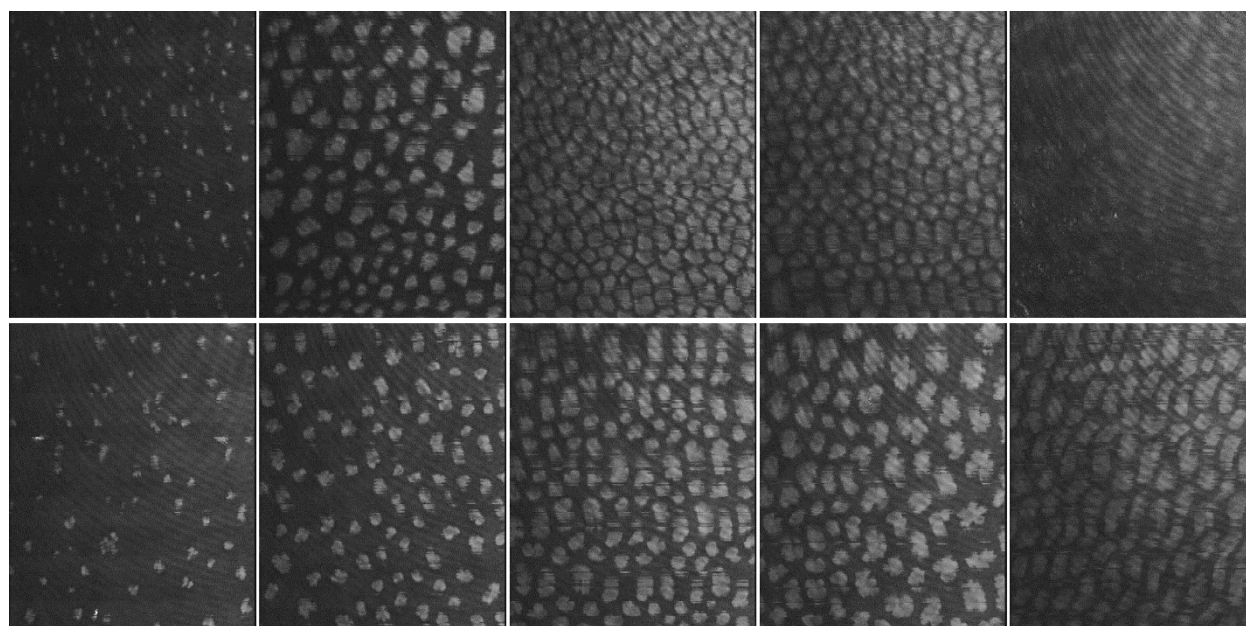


**Figure 2.3. BAM images (220 nm width) of surface pressures (left to right):  $10 \text{ mNm}^{-1}$ ,  $20 \text{ mNm}^{-1}$ ,  $25 \text{ mNm}^{-1}$ ,  $30 \text{ mNm}^{-1}$  and  $40 \text{ mNm}^{-1}$  of DPPC:POPG on water (top) and TBS (bottom).**

For DPPC:POPG:PA (Fig. 2.4), there is a clear change in domain size and shape with the addition of buffer at all surface pressures which is not observed with DPPC:POPG alone. The line tension is significantly lower in the absence of buffer leading to flower shaped domains. GIXD has shown that PA interacts with DPPC to form a mixed crystalline condensed phase on water<sup>41</sup>. Since the carboxylic acid headgroups of PA are deprotonated on both subphases used, the presence of salt may affect domain morphology due to a counterion effect. Similar to the DPPC:POPG system, at pressures above 20 mNm<sup>-1</sup>, the film is more expanded on TBS than on water both in the images and the isotherms. Moreover, domains clearly start forming at lower pressures (note the domain density difference at 10 mNm<sup>-1</sup> and the lowered plateau in the isotherm) and the LE phase squeezed out earlier on the water subphase. Similar to the DPPC:POPG system, the later squeeze-out of the LE phase could be due to the stabilization of charge repulsion by the sodium cations.

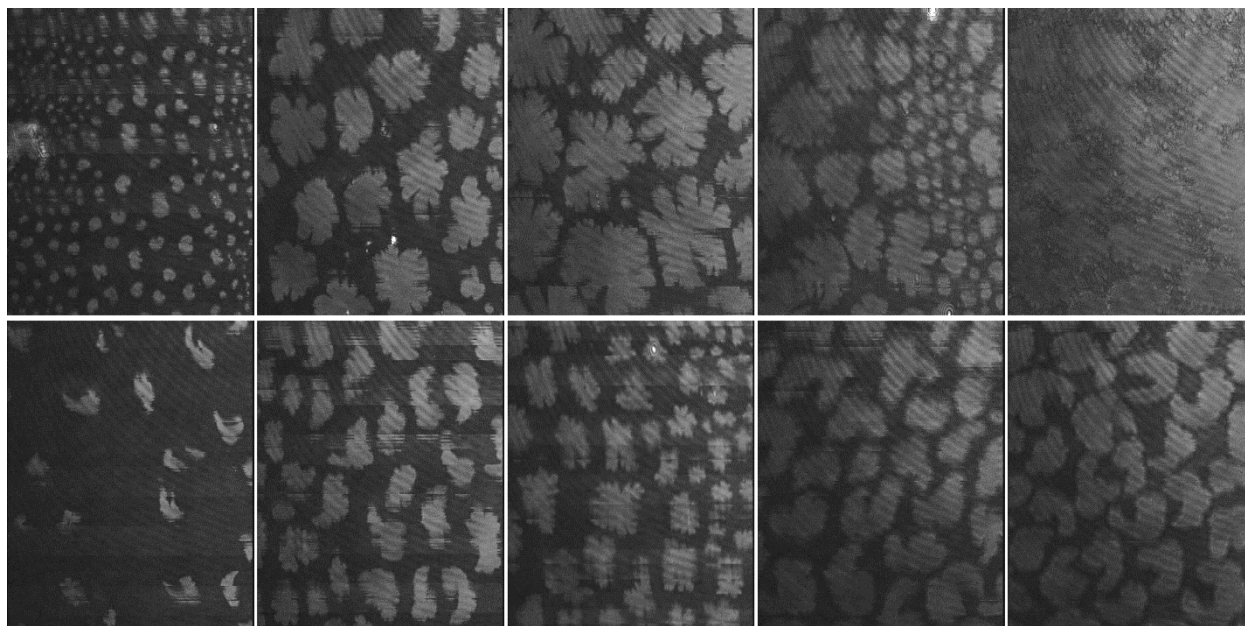


**Figure 2.4. BAM images (220 nm width) of surface pressures (left to right): 10 mNm<sup>-1</sup>, 20 mNm<sup>-1</sup>, 25 mNm<sup>-1</sup>, 30 mNm<sup>-1</sup> and 40 mNm<sup>-1</sup> of DPPC:POPG:PA on water (top) and TBS (bottom).**

On the other hand, the BAM images of Infasurf on water and on TBS show very little difference (Fig. 2.5). Both also have LE phase squeeze-out at around  $40 \text{ mNm}^{-1}$ . Comparing the BAM images for Infasurf to those of DPPC:POPG (Fig. 2.3), the differences in domain size and in line tension due to the presence of the cationic SP-B protein are more pronounced when the subphase is buffered, however the underlying differences seem to occur in the lipid films.

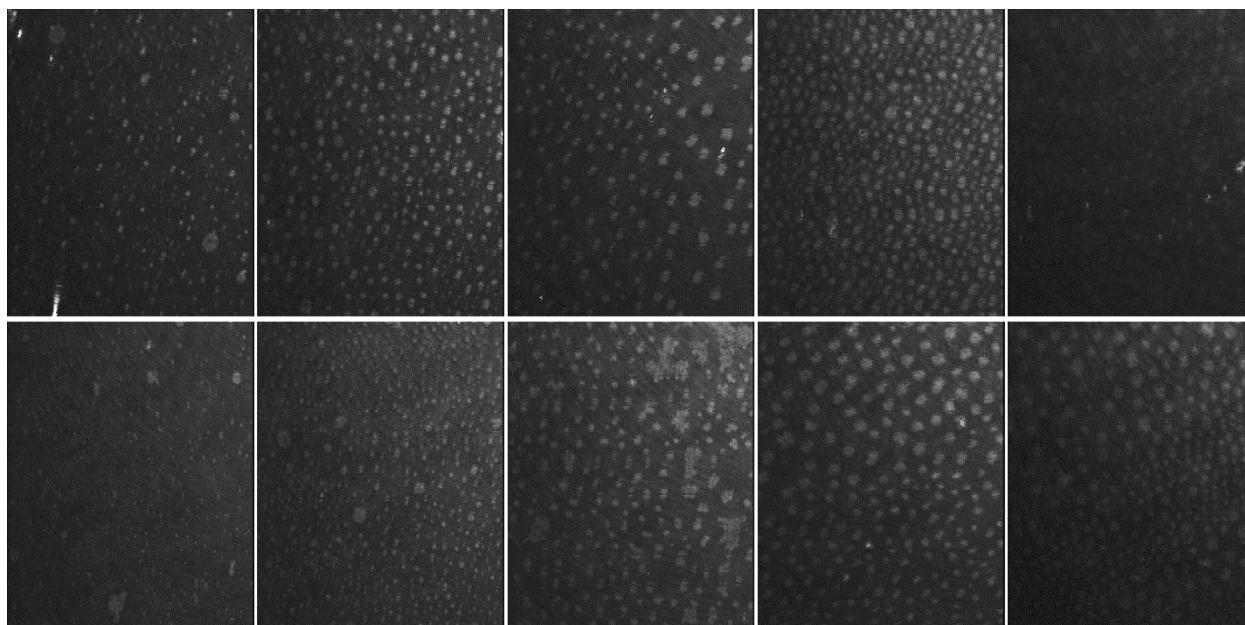


**Figure 2.5.** BAM images (220 nm width) of surface pressures (left to right):  $10 \text{ mNm}^{-1}$ ,  $20 \text{ mNm}^{-1}$ ,  $25 \text{ mNm}^{-1}$ ,  $30 \text{ mNm}^{-1}$  and  $40 \text{ mNm}^{-1}$  of Infasurf on water (top) and TBS (bottom).

Survanta, which contains the additional palmitic acid, low in SP-B and rich in SP-C protein, exhibits smaller domains on the water subphase but otherwise similar behavior in the presence or absence of buffer. More striking is the comparison of DPPC:POPG:PA to Survanta which exhibits a clear reduction in domain size when SP-C is present. Moreover, at  $40 \text{ mNm}^{-1}$ , the LE phase is never completely squeezed out. Contrary to Infasurf, where there appears to be only some residual LE phase present, in Survanta, the LE phase is quite apparent. Thus SP-C, the dominant surfactant protein present in Survanta, may act to maintain the LE phase at the interface. Also, because of the similarity at  $40 \text{ mNm}^{-1}$  for Survanta on either water or TBS, it appears that SP-C is not affected very much by the presence of salt.

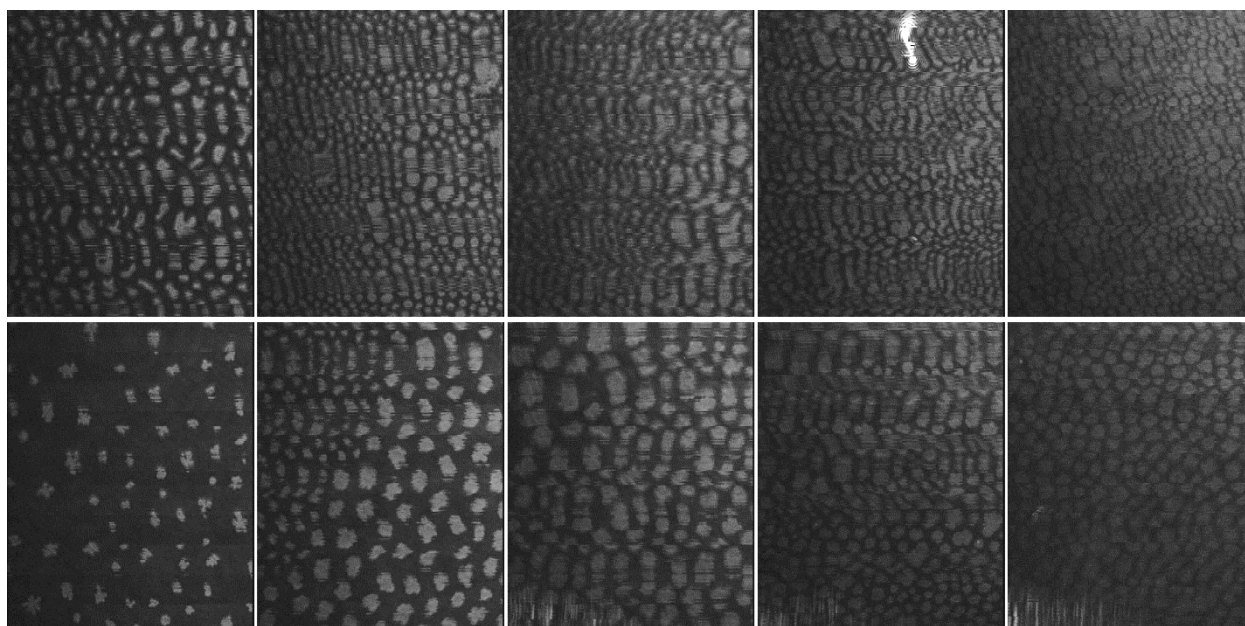


**Figure 2.6. BAM images (220 nm width) of surface pressures (left to right):  $10 \text{ mNm}^{-1}$ ,  $20 \text{ mNm}^{-1}$ ,  $25 \text{ mNm}^{-1}$ ,  $30 \text{ mNm}^{-1}$  and  $40 \text{ mNm}^{-1}$  of Survanta on water (top) and TBS (bottom).**

It is known that both surface dilational elasticity and viscosity are higher in systems with saturated lipids since they can pack together to form a condensed phase <sup>74</sup>. Therefore, when a system is more fluid, it is expected that elasticity and viscosity will be reduced. Thus far, through compression isotherms and BAM images, it has been shown that buffering the subphase, makes the film more fluid. Similarly, the elasticity and viscosity of DPPC:POPG, are both reduced when using TBS (Fig. 2.7). The reduction in viscoelastic properties are more evident after the DPPC phase transition (LE to C) at approximately 15 mNm<sup>-1</sup> where the impact of the increased proportion of LE phase is more apparent (below this pressure the entire film forms a LE phase). In particular the LE-C phase transition manifests itself as a maximum in the viscosity due to a near zero slope at the transition and a slope change in the elasticity both of which highlight that the LE-C phase transition occurs at a higher pressure on buffer.

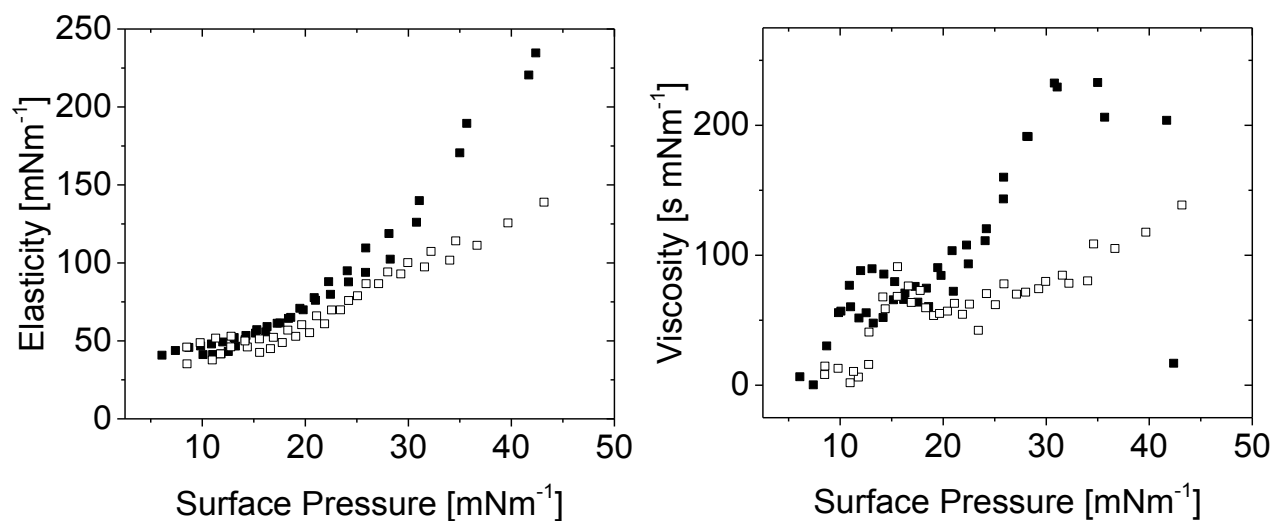


**Figure 2.7. Surface dilational elasticity (left) and viscosity (right) data of DPPC:POPG on water (■) and TBS (□).**

The same can be observed for the DPPC:POPG:PA system in Figure 2.8, where going from water to TBS decreases the films rheological properties due to the presence of more LE phase. In this case the LE-C phase transition pressure is reduced to approximately 10 mNm<sup>-1</sup>. However, it should be noted that the presence of PA increases the film's rheological properties due to closer packing of the film <sup>41</sup>.

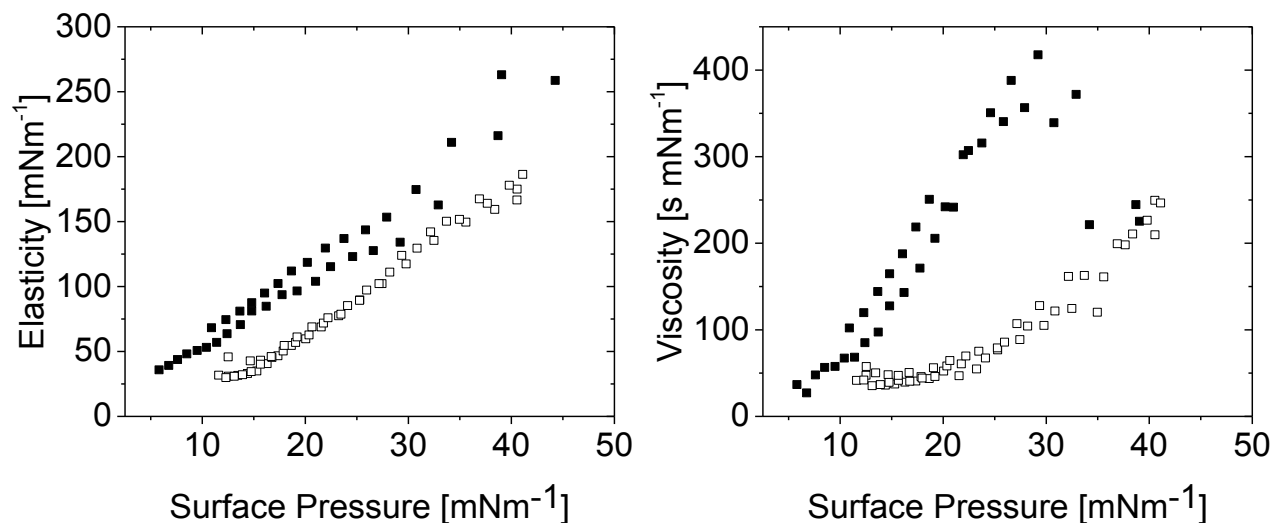


**Figure 2.8.** Surface dilational elasticity (left) and viscosity (right) data of DPPC:POPG:PA on water (■) and TBS (□).

For Infasurf, the subphase does not have a major impact on the viscoelastic properties (Fig. 2.9). Although the isotherm shows an expansion, BAM images indicate that up to  $40 \text{ mNm}^{-1}$  there is very little change in morphology and the LE phase is always present. This system contains cationic proteins which may already interact with the charged phospholipids in a manner which reduces the impact of salt screening.

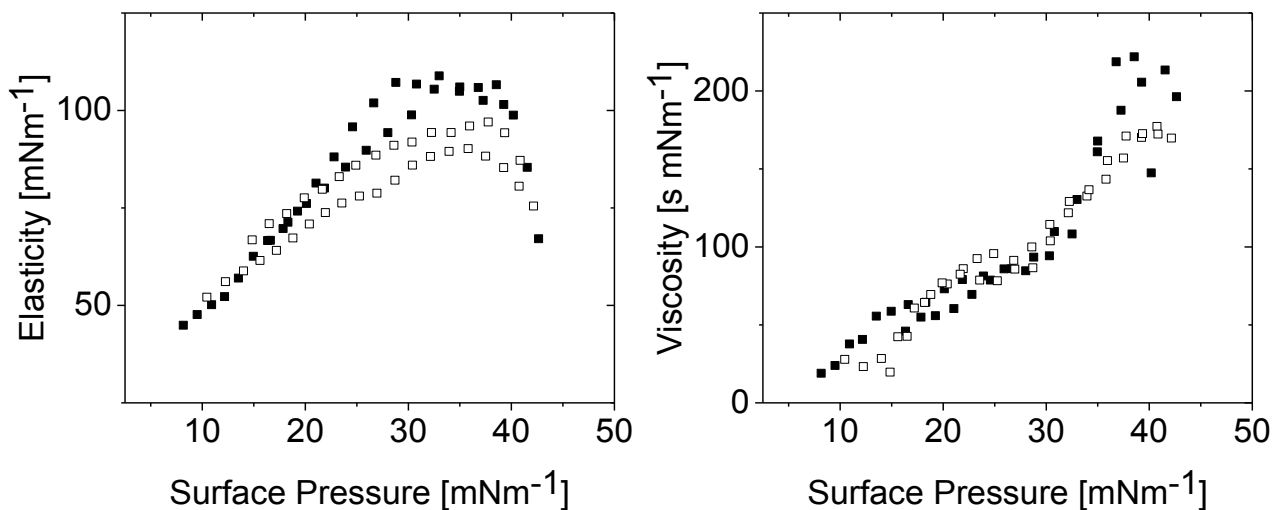


**Figure 2.9.** Surface dilational elasticity (left) and viscosity (right) data of Infasurf on water (■) and TBS (□).

On the other hand, the rheological properties for Survanta shown in Figure 2.10, are evidently reduced when using a TBS subphase rather than water. Survanta, like Infasurf, is also

always in the LE phase. However, there are two noteworthy differences: the presence of the PA additive and the low proportion of SP-B. The PA significantly increases the viscoelastic properties of the system and thus any reduction may be amplified. Conversely, for Infasurf the moderating effect of the protein already lowers the viscoelastic properties significantly and therefore any reduction may be difficult to discern. The PA may also undergo redistribution between the phases with greater charge screening. Finally, the lack of the charged SP-B may leave the film more susceptible to the effects of ionic strength and counterions.

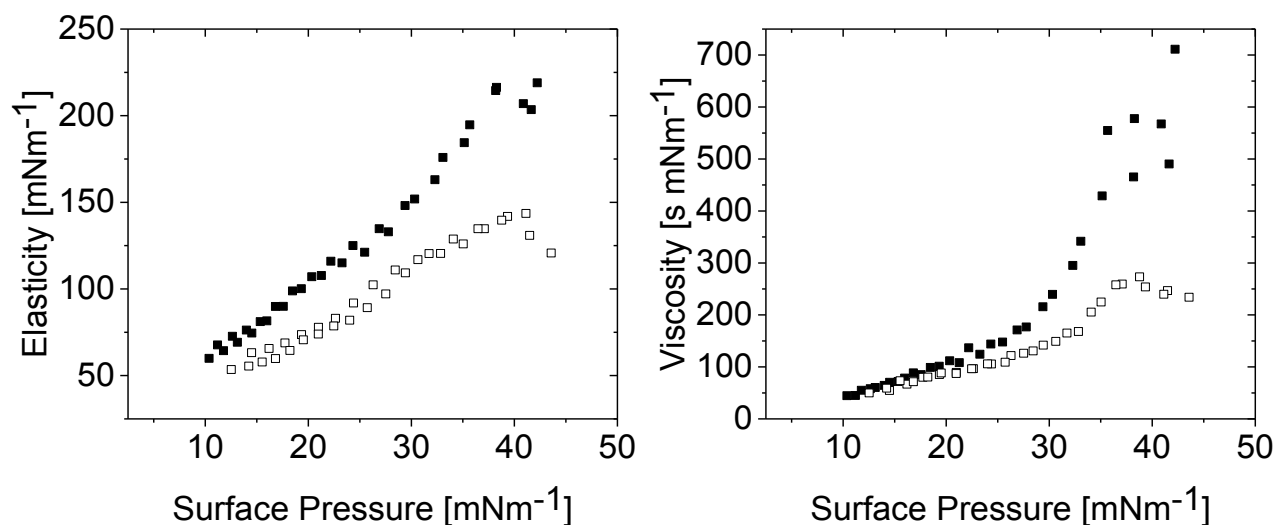


**Figure 2.10. Surface dilational elasticity (left) and viscosity (right) data of Survanta on water (■) and TBS (□).**

GIXD was used to evaluate structural changes in the condensed phase of the monolayers. Figure 2.11 shows a plot of the scattered intensity as a function of the in-plane ( $Q_{xy}$ ) and out-of-plane ( $Q_z$ ) components for DPPC:POPG:PA. Fitted peak positions for all systems are presented in Table 2.1 and the resulting lattice and chain tilt parameters in Table 2.2 (a figure showing the unit cell is provided in Appendix A, Fig. A3). Both lipid only systems exhibit three peaks all at values of  $Q_z > 0$  which corresponds to an oblique chain lattice with a tilt azimuth between nearest neighbor (NN) and next nearest neighbor (NNN). Both systems show a pronounced expansion of the unit cell on a buffered subphase leading to an increased tilt angle of the chain which correlates with the reduced viscoelastic parameters. This effect is greater with the PA present and may indicate the higher impact of counterions on a condensed phase containing a charged species.

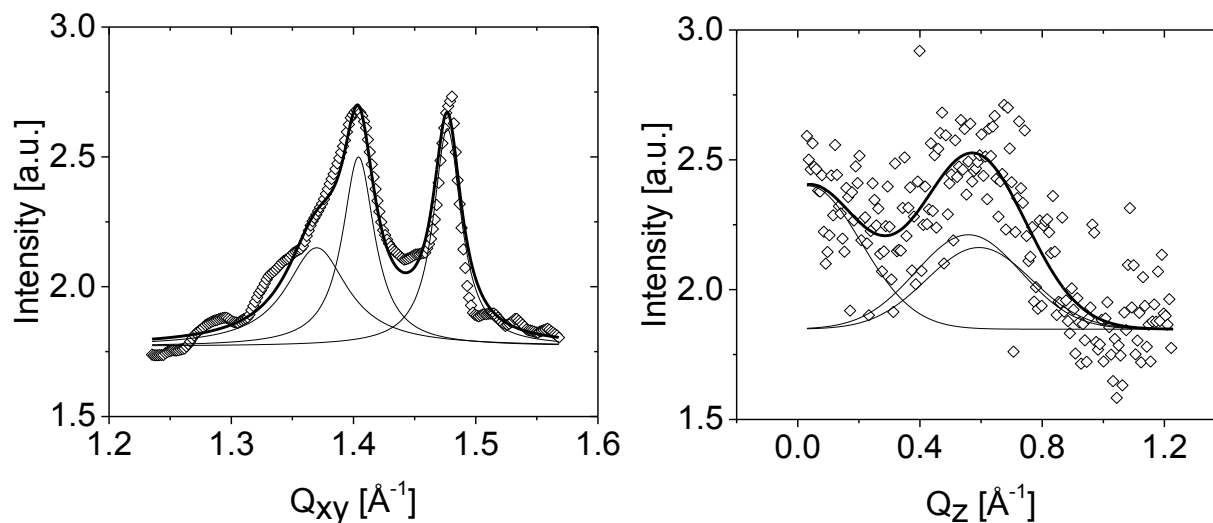


Figure 2.11.  $Q_{xy}$  (left) and  $Q_z$  (right) fit peaks of DPPC:POPG:PA at  $25 \text{ mNm}^{-1}$  on TBS.

Table 2.1.  $Q_{xy}$  and  $Q_z$  of DPPC:POPG, DPPC:POPG:PA, Infasurf and Survanta

System		Pressure [ $\text{mNm}^{-1}$ ]	$(1 \pm 1) [\text{\AA}^{-1}]$		$(01) [\text{\AA}^{-1}]$		$(10) [\text{\AA}^{-1}]$	
			$Q_{xy}$	$Q_z$	$Q_{xy}$	$Q_z$	$Q_{xy}$	$Q_z$
Water	DPPC:POPG <sup>41</sup>	35	1.479	0.08	1.439	0.40	1.409	0.48
Buffer	DPPC:POPG	35	1.474	0.09	1.422	0.52	1.366	0.60
Water	DPPC:POPG:PA <sup>41</sup>	25	1.486	0.07	1.462	0.38	1.435	0.45
Buffer	DPPC:POPG:PA	25	1.476	0.03	1.404	0.56	1.370	0.59
Water	Infasurf	45	1.506	0.13	1.477	0.015	1.437	0.11
Buffer	Infasurf	45	1.507	0.17	1.482	0.042	1.432	0.13
Water	Survanta <sup>4</sup>	20	1.482	0.11	1.454	0.35	1.428	0.45
Buffer	Survanta <sup>42</sup>	20	1.480	0	-	-	1.440	0.41
Water	Survanta <sup>4</sup>	30	1.489	0	-	-	1.475	0.25
Buffer	Survanta <sup>42</sup>	30	1.490	0	-	-	1.470	0.23

Infasurf tilt angle measurements presented in Table 2.2 are at  $45 \text{ mNm}^{-1}$ . This is because the area occupied by condensed phase in the footprint region of the x-ray beam is much lower in

the lipid-protein systems and therefore yield much weaker peaks. For this reason, for a good fit, it was necessary to do the analysis at a higher pressure where more of the LE phase is squeezed out. Again, an oblique lattice is observed, however, Infasurf exhibits only a small change in tilt angle when comparing water and buffer which correlates well with the relatively small decrease in viscoelasticity. However, it is important to note that the peaks were weaker on water than on buffer. Also, there were very weak additional peaks at low  $Q_{xy}$  values which we believe may be due to a liquid ordered (LO) phase due to the presence of cholesterol in Infasurf<sup>11</sup> but they were too weak to fit. The minimal change in tilt angle observed for Infasurf can be due to the amount of SP-B present which may already serve as a counterion in the film. Moreover, it must be noted that the elasticity and viscosity values (Fig. 2.9) are already low on water that the relative difference may be minimal when compared to buffer.

GIXD data for Survanta is available in the literature and this system was not re-measured. Unit cell parameters were calculated based on the data available and are included in the table for comparison. Survanta also exhibits small differences in tilt angle based on the subphase used. However it appears that the tilt angle is decreasing when comparing water to buffer. It is not clear why the GIXD measurements show the film to be more contracted on buffer but some factors to consider are: the complexity of the condensed phase since there are many different lipids present in biological systems, the presence of protein and the use of a sodium bicarbonate saline buffer in the data source<sup>75</sup> instead of TBS. To explore the behavior of Survanta further, we propose to take GIXD measurements with our own systems using the same conditions as for Infasurf and using the same extract as for the rest of the data to take compositional differences into account. Another possible explanation for this decrease is that the use of buffer has led to an earlier transition from an oblique lattice (three peaks at  $Q_z > 0$ ) to a centered rectangular unit cell with NN tilt (Table 2.1, two peaks a non-degenerate peak at  $Q_z = 0$  and a degenerate peak at  $Q_z > 0$ ). Given that the viscosity decreases dramatically similar to some of the other systems and the phase dominated by the anionic lipid, POPG, is the LE phase it is likely that the buffer impact on this phase dominates the rheology.

**Table 2.2. Lattice Parameters (a, b,  $\gamma$ ), chain tilt (t), area per chain perpendicular to the chain long axis ( $A_0$ ) and the projected area per chain ( $A_{xy}$ ) of DPPC:POPG, DPPC:POPG:PA, Infasurf and Survanta**

	System	Pressure [mNm <sup>-1</sup> ]	a [Å]	b [Å]	$\gamma$ [°]	t [°]	$A_{xy}$ [Å <sup>2</sup> ]	$A_0$ [Å <sup>2</sup> ]
Water	DPPC:POPG <sup>41</sup>	35	4.92	5.02	117.4	20.3	21.9	20.6
Buffer	DPPC:POPG	35	4.92	5.13	116.2	25.8	22.7	20.4
Water	DPPC:POPG:PA <sup>41</sup>	25	4.88	4.97	118.3	18.8	21.4	20.2
Buffer	DPPC:POPG:PA	25	4.97	5.09	115.7	26.4	22.8	20.4
Water	Infasurf	45	4.81	4.94	117.8	5.21	21.0	21.0
Buffer	Infasurf	45	4.80	4.96	117.7	6.85	21.0	20.9
Water	Survanta <sup>4</sup>	20	4.90	4.99	118.1	19.0	21.6	20.5
Buffer	Survanta <sup>42</sup>	20	5.09	4.95	120.9	18.4	21.6	20.5
Water	Survanta <sup>4</sup>	30	4.93	4.89	120.3	11.1	20.8	20.4
Buffer	Survanta <sup>42</sup>	30	4.96	4.90	120.5	10.3	20.9	20.6

All of these values were calculated from  $Q_{xy}$  and  $Q_z$  values reported in the literature or our own measurements. The chain tilt (t) is the angle of the fully extended alkyl chain relative to the normal.

In terms of model LS membrane composition, systems with PA always reach higher rheological values than systems without PA whether counterions are present or not. However, systems with surfactant proteins behave differently when salt is present. For example, in terms of elasticity, at low surface pressures Infasurf and Survanta exhibit similar values only when salt is present (Appendix A, Fig. A4 & A5). In the case of viscosity, the lipid-only (DPPC:POPG, DPPC:POPG:PA) systems exhibit greater viscosity values than their comparable lipid-protein (Infasurf, Survanta) counterparts on water, but, the opposite occurs on buffer.

## 2.5. Conclusion

Overall, the lipid-only films (DPPC:POPG, DPPC:POPG:PA) appear to be more expanded when salt is present in the subphase. This is corroborated with compression isotherms, BAM

images, rheological and GIXD measurements. This film expansion may be attributed to intercalation of sodium cations between the anionic POPG headgroups which may also stabilize charge repulsion to prevent earlier squeeze-out (BAM) as seen with only water. A similar interaction may be occurring with the deprotonated carboxylic acid headgroups of PA and the sodium cations.

The lipid-protein systems are more complicated in terms of both composition and behaviour. Firstly, Infasurf appears to be more expanded based on compression isotherms on TBS, but does not exhibit significant changes in morphology and rheology. Also, GIXD measurements do show a slightly more expanded film but it also appears to show the existence of another phase which may be due to the presence of cholesterol. These findings could be due to the presence of the cationic SP-B that may be minimizing the impact of the buffer seen with the lipid-only systems. This emphasizes the need for physiological conditions if the proteins are to achieve their full role and function in the model system. In the case of Survanta, compression isotherms indicate a more expanded film on a buffer subphase which correlates with the reduction in viscoelastic properties. Like Infasurf, BAM images do not exhibit a great deal of change although in contrast to Infasurf, Survanta appears to maintain the LE phase at the interface at higher pressures which may be due to the high proportion of SP-C present in comparison to SP-B. GIXD measurements should be done using the same conditions (i.e. TBS, same batch number for the bovine extract) as was done for Infasurf since the results from the literature point to a decrease in tilt angle going from water to buffer implying a contraction of the film. This work outlines the importance of using a physiologically relevant buffer in LS studies and highlights the differences in the biophysical properties of model LS films induced by subphase composition.

## Chapter 3. Biophysical Impacts of Ozone Exposure on Model Lung Surfactant Films

This manuscript has been prepared for submission to *Langmuir* with the following authorship: Sahana Selladurai, Rolf Schmidt and Christine DeWolf.

### 3.1. Abstract

The exposure of four model lung surfactant systems to the atmospheric pollutant ozone was studied. These systems included two lipid-only (synthetic lipid mixtures comprising saturated and unsaturated phospholipids with or without added palmitic acid) and two lipid-protein (natural lung surfactant extracts) systems. Exposure of all systems to ozone showed a lower squeeze-out pressure and the lipid-only systems additionally showed a shift in the isotherm to higher molecular areas attributed to accommodation of the cleaved phospholipid chain at the interface. The earlier squeeze-out was visualized for the phospholipid-only system (dipalmitoylphosphatidylcholine, DPPC, and 1-palmitoyl-2-oleyl-phosphatidylglycerol, POPG) using Brewster angle microscopy although no other significant changes to morphology were observed upon exposure to ozone. On the other hand, all systems, with the exception of the phospholipid-only system, exhibited reductions in viscoelastic parameters, namely film dilational viscosity and elasticity. Thus ozone exposure is demonstrated to have a significant impact on physicochemical properties essential for lung surfactant functioning.

### 3.2. Introduction

Lung surfactant (LS) is a monolayer film at the air-liquid interface of the lung that serves to reduce surface tension to prevent alveolar collapse and reduce the work necessary for breathing<sup>1-4</sup>. It is composed of saturated and unsaturated phospholipids, neutral lipids such as cholesterol and surfactant proteins A, B, C and D<sup>2,5-7</sup>. Lung surfactant comes into direct contact with the air we breathe and can be directly affected by atmospheric pollutants such as ground-level ozone. Ozonolysis can affect multiple components of lung surfactant including unsaturated phospholipids and amino acid residues present in surfactant proteins.

Annual medians of tropospheric ozone concentrations from 1988 to 2001 were found to be approximately 30 ppb with annual maxima ranging from 60 – 116 ppb and in 2004, annual medians

ranging from 23 – 34 ppb across Canada <sup>76,77</sup>. Highly polluted air has been associated with ozone concentrations of greater than 300 ppb <sup>77</sup>. Long-term exposure to ambient levels of tropospheric ozone have been linked to decreased lung function in adolescence and increased airway inflammation in asthmatics <sup>55,56</sup>; LS may also be affected by ambient levels of ground-level ozone since it is the primary contact point between the atmosphere and the rest of the lung.

Lung surfactant replacement therapies can be used as models to study the effect of atmospheric pollutants. These therapies are clinically used to treat premature babies with respiratory distress syndrome <sup>37</sup>. The most common form of lung surfactant replacement therapies are derived from animals such as the bovine, the preparation of which involves removal of SP-A and SP-D since these are not surface-active and provide an immunological role <sup>5</sup>. SP-B and SP-C are surface-active and are involved in membrane-membrane associations and reservoir formation respectively <sup>8-10</sup>. Therefore, oxidation of these proteins by ozone may impact their ability to perform these roles.

To understand the impact of ozone exposure on lung surfactant as a function of composition, four model systems are studied: DPPC:POPG, DPPC:POPG:PA, Infasurf and Survanta. Infasurf and Survanta are lung surfactant replacement therapies derived from the bovine. DPPC and POPG are commonly used to represent the saturated and unsaturated lipid components of lung surfactant, respectively. DPPC:POPG:PA is used to study the effect of the addition of palmitic acid to make the link to Survanta which contains added PA along with SP-C and SP-B. DPPC:POPG serves as the comparison to Infasurf which contains saturated and unsaturated phospholipids along with SP-B and SP-C but no additives. Survanta and Infasurf are compared to see the influence of the different proteins as Survanta is low in SP-B (approximately 0.04 %w/w SP-B and 0.9 %w/w SP-C) and Infasurf is enriched in SP-B (approximately 0.9 %w/w SP-B and 0.7 – 1.3 %w/w SP-C) <sup>11</sup>. The effect of ozone exposure on these four model lung surfactant membranes was studied using both buffer and water as the subphase. However, the focus here will be the physiologically relevant buffer which has been shown previously to have an impact on both morphology and rheology (Chapter 2). Lung surfactant contains both unsaturated phospholipids and surfactant proteins that contain potentially oxidizable amino acids, both of which are essential for its physicochemical properties and proper functioning *in vivo*. The impact of ozone exposure on surface activity, morphology and rheology are discussed here.

### 3.3. Materials & Methods

**Materials.** Dipalmitoylphosphatidylcholine (DPPC, > 99 %) and 1-palmitoyl-2-oleoyl-phosphatidylglycerol (POPG, > 99 %) were purchased from Avanti Polar Lipids. Palmitic acid (PA, > 99 %), tris(hydroxymethyl)aminomethane (tris, > 99.8 %), NaCl salt (> 99 %) and phosphate-buffered saline tablets (PBS, pH 7.4, 10 mM phosphate, 137 mM NaCl, 2.7 mM KCl) were all purchased from Sigma-Aldrich. Survanta and Infasurf are lung surfactant replacement therapies that were donated by Abbott Laboratories and Ony Inc. respectively. The spreading solvent used in all experiments conducted was HPLC grade chloroform obtained from Fisher Scientific.

**Preparation of Mixtures, Solutions & Subphases.** The DPPC:POPG and the DPPC:POPG:PA mixtures were prepared using stock solutions of DPPC, POPG, and PA to achieve molar ratios of 77:23 and 61:19:20 respectively, all of which were prepared in chloroform. The Infasurf and Survanta solutions were prepared by introducing weighed lyophilized sample into chloroform. Water subphases comprised of Ultrapure water with a resistivity of  $18.2 \text{ M}\Omega \text{ cm}^{-1}$  from a Barnstead Easypure II LF purification system. The tris-buffered saline (TBS) was prepared by using 50 mM tris and 150 mM NaCl in ultrapure water, where the pH was adjusted to 7.4 using hydrochloric acid.

**Surface Activity and Rheology.** Surface activity and rheological measurements were carried out using a SINTERFACE Technologies profile analysis tensiometer (PAT), where a model lung surfactant monolayer solution in chloroform with a concentration of less than  $0.1 \text{ mg mL}^{-1}$  was spread on a  $10 \mu\text{L}$  drop of subphase. The subphase for all experiments comprised either ultrapure water or tris buffered saline as previous work has highlighted the importance of a physiologically relevant buffer (Chapter 2). The spreading volume ranged from  $0.4$  to  $0.8 \mu\text{L}$ . After spreading, the surface area of the pendant drop was expanded from  $25$  to  $40 \text{ mm}^2$ . The drop was then left to equilibrate for an additional 3 minutes to allow for complete evaporation of the chloroform and possible rearrangement of the membrane components. For surface activity measurements, surface pressure-area isotherms were obtained using a molecular compression speed of  $0.06 \text{ mm}^2\text{s}^{-1}$ . Rheological measurements were made by sequential measurements along the compression isotherm for duplicate films as outlined in Figure 2.1. From the initial surface area of  $40 \text{ mm}^2$  the film is compressed to  $26.8 \text{ mm}^2$  at a compression speed of  $0.06 \text{ mm}^2\text{s}^{-1}$ , the drop was then left to equilibrate for 300 s after which the drop volume was oscillated for 600 s

with an amplitude of  $0.5 \text{ mm}^2$ , and a frequency of  $0.01 \text{ s}^{-1}$  (100 s period, 6 oscillations). The drop was then left to equilibrate for 180 s, before compressing to the next surface area, equilibrated (300 s) and oscillated once again using the same parameters. This cycle was continued until a surface tension of around  $25 \text{ mNm}^{-1}$  was reached, giving rheological data for surface pressures ranging from 10 to  $45 \text{ mNm}^{-1}$ . This rheological data yields the dilational surface elasticity and viscosity of the monolayer <sup>72</sup>.

Ozone exposure experiments were carried out by first compressing the monolayer spread at the air-liquid interface of the drop to the desired surface area and then by exposing the drop to an ozone concentration of 800 ppb in a 40 mL reaction chamber with a flow rate of  $100 \text{ mLmin}^{-1}$  30 minutes prior to the first rheology measurement using the same method as above. A UVP ozone generator, a 2B Technology ozone monitor and an Aalborg digital mass flow controller were used to generate the ozone and control the flow.

**Brewster Angle Microscopy.** Brewster angle microscopy (BAM) was performed on films spread from a concentration of less than  $1.0 \text{ mg mL}^{-1}$  in chloroform on a Langmuir film balance (NIMA technology) coupled with an I-Elli2000 imaging ellipsometer (i-Elli2000, Nanofilm Technologies). This instrument is equipped with a 50 mW Nd:YAG laser ( $\lambda = 532 \text{ nm}$ ) and images were obtained using a 20X magnification lens with a lateral resolution of  $1 \text{ }\mu\text{m}$  and a  $53.15^\circ$  incident angle. For these films, a compression speed of  $5 \text{ cm}^2 \text{ min}^{-1}$  was used.

For ozone exposure of films on the Langmuir trough (for BAM measurements), the Teflon trough was enclosed using a Plexiglas cover with an inlet and outlet at either end for gas flow using the same parameters as above.

### 3.4. Results & Discussion

Compression isotherms of all four systems are presented in Figure 3.1; all of which exhibit a lowered squeeze-out pressure. Previous work has demonstrated that ozone exposure of unsaturated phospholipid films produces aldehydes, carboxylic acids and peroxides <sup>60</sup>. The lipid-only systems exhibit a shift to greater molecular area after ozone exposure which is attributed to accommodation of the cleaved POPG chain <sup>62</sup> (and therefore an expansion of the film). However, in the case of the lipid-protein systems, Infasurf and Survanta, little to no shift is observed after ozone exposure. Contrary to the lipid-only systems, Survanta and Infasurf also contain polyunsaturated lipids that become significantly less surface active after oxidation (due to cleavage

into much smaller, more polar fragments) leading to a contraction of the film. These systems also contain surfactant proteins that can be affected by oxidation. The amino acid sequence of a protein is responsible for its secondary and tertiary structure; oxidation of certain amino acid residues may lead to alteration of the structure and thus the protein function. Cysteine, methionine, tryptophan, tyrosine, histidine and phenylalanine are all oxidizable amino acid residues, where tryptophan is the most sensitive to oxidation <sup>78</sup>. Bovine SP-B has 14 oxidizable residues and SP-C has 4 <sup>79</sup>. Amino acid oxidation has been shown to affect different properties, for example, oxidation of cysteine may lead to changes in a protein's specific optical rotation and oxidation of tryptophan, methionine and tyrosine may lead to increased flexibility or rigidity in that region of the protein thereby altering the protein's structure <sup>78</sup>. Taking into account the effect of oxidation of POPG, polyunsaturated lipids and the surfactant proteins, there are many different factors influencing possible shifts in the compression isotherms of lung surfactant replacement therapies after ozone exposure, i.e. the lack of shift may be due to competing influences. Oxidation of Survanta films by environmental tobacco smoke resulted in a significant thinning of the liquid expanded phase relative to unexposed films <sup>43</sup>, supporting a reorientation of the cleaved fragments to be able to contact the subphase.

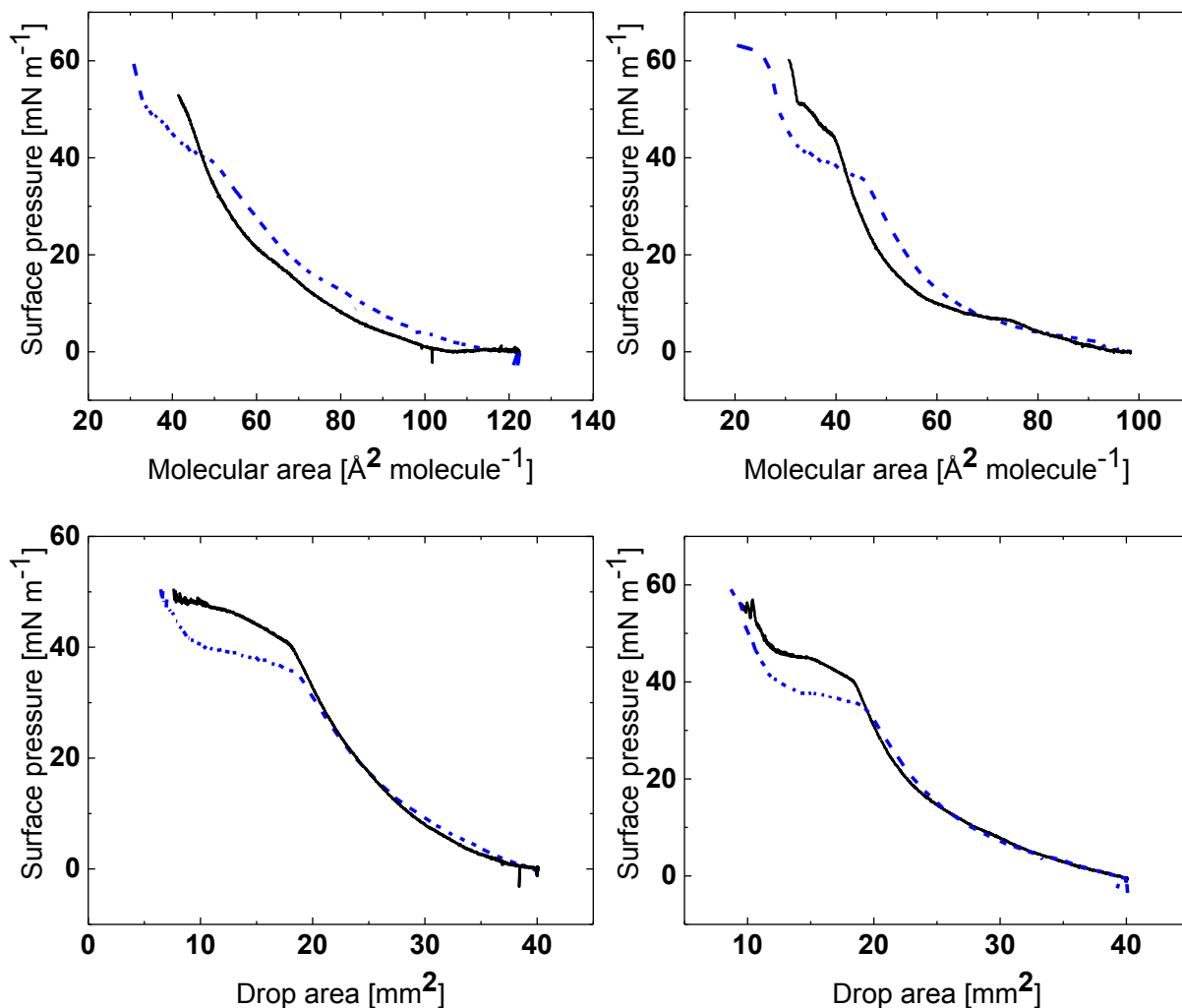


**Figure 3.1. Isotherms of DPPC:POPG (top, left) , DPPC:POPG:PA (top, right), Infasurf (bottom, left) and Survanta (bottom, right) monolayers before ozone exposure (–) and after ozone exposure (– –) at 23°C. Note that the isotherms of the lipid-protein systems are plotted as a function of drop area as the average molecular weight is unknown for natural extracts.**

BAM images of the DPPC:POPG system (Fig. 3.2) show little change in morphology up to 30 mNm<sup>-1</sup> after ozone exposure in comparison to the pre-ozone exposure films. From 30 mNm<sup>-1</sup>, there is a clear early squeeze-out of LE phase from the surface. This is because of increased solubility of the reacted POPG and the lack of surfactant proteins to maintain a LE phase. With the addition of PA (Fig. 3.3), the only difference after ozone exposure is the slight changes in line tension at 10 and 20 mNm<sup>-1</sup>. The presence of PA in general increases the squeeze-out pressure to above 40 mNm<sup>-1</sup>, thus squeeze-out is not observed either before or after ozone exposure using BAM due to limitations on the available trough area. Survanta behaves similarly to the DPPC:POPG:PA system after ozone exposure. In the BAM images (Fig. 3.5), as with the

DPPC:POPG:PA system, there are some changes in line tension after ozone exposure at 10 and 20  $\text{mNm}^{-1}$ . Since PA itself is not oxidized by ozone over this timeframe, as noted by the electro-spray ionization mass spectrometry (ESI-MS, Appendix A, Fig. A8 & A9) results and previously shown for stearic acid<sup>80</sup>, this suggests that the oxidation of the POPG affects the line tension between the liquid expanded and liquid condensed phases only in the presence of PA. Furthermore, no squeeze-out is observed with Survanta. While this may be the impact of PA, as noted above, it is also likely that the surfactant proteins maintain a liquid expanded phase in the monolayer even after squeeze-out as this behaviour is also noted for Infasurf<sup>25</sup>. Both the DPPC:POPG:PA and Survanta systems exhibit some collapsed material at and above 30  $\text{mNm}^{-1}$  that is not observed with either DPPC:POPG or Infasurf. The presence of early collapsed material after ozone exposure seems to be due to PA, where pure PA films have been shown to collapse at pressures before 40  $\text{mNm}^{-1}$ <sup>4</sup>. BAM images of Infasurf (Fig. 3.4) also do not exhibit a significant difference before and after ozone exposure within 40  $\text{mNm}^{-1}$  which may be because the pressure range was not high enough or due to the maintenance of the LE phase at the surface by the surfactant proteins.

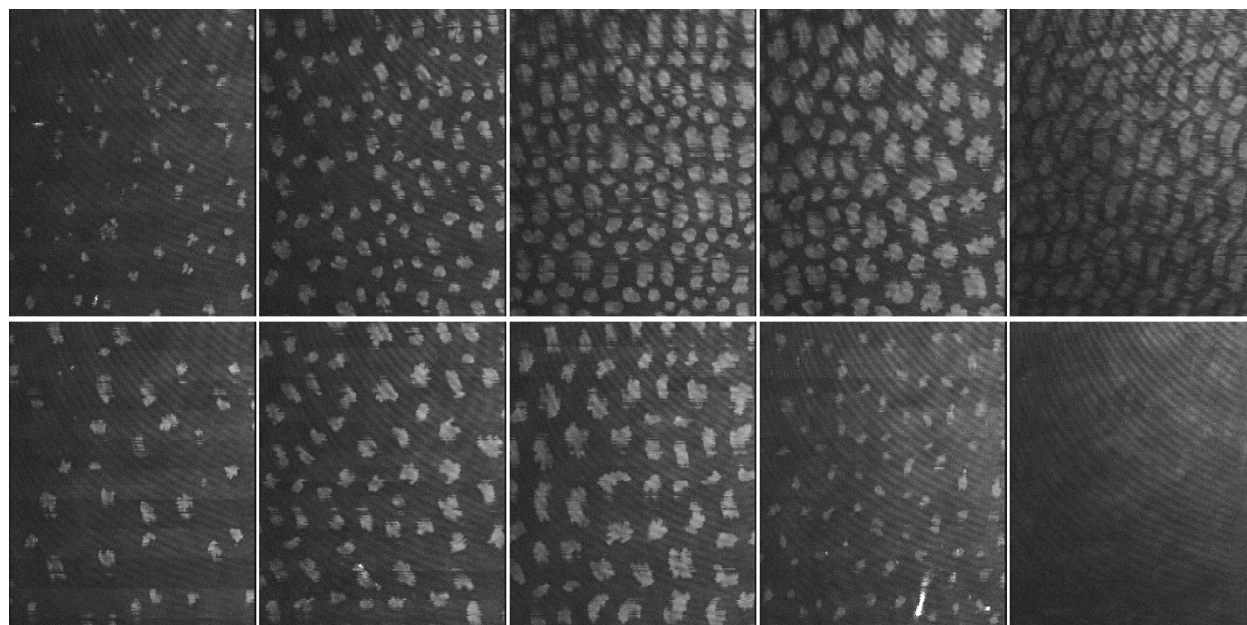


**Figure 3.2. BAM images (220 nm width) of surface pressures (left to right): 10  $\text{mNm}^{-1}$ , 20  $\text{mNm}^{-1}$ , 25  $\text{mNm}^{-1}$ , 30  $\text{mNm}^{-1}$  and 40  $\text{mNm}^{-1}$  of DPPC:POPG before ozone exposure (top) and after ozone exposure (bottom).**

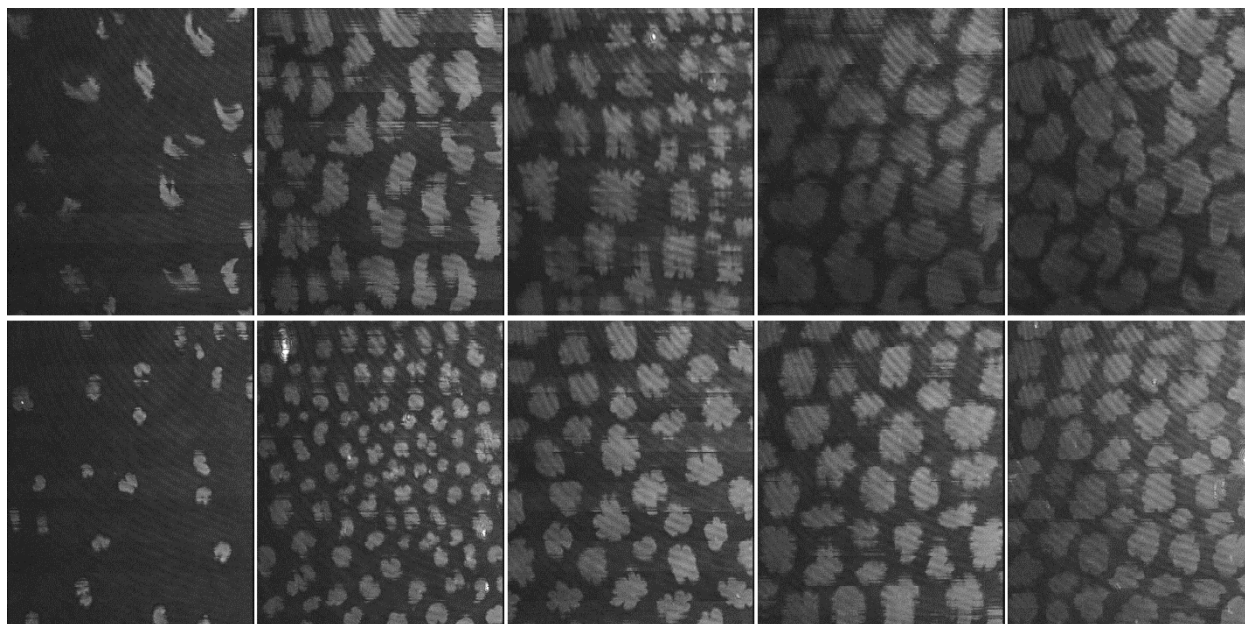


**Figure 3.3.** BAM images (220 nm width) of surface pressures (left to right): 10 mNm<sup>-1</sup>, 20 mNm<sup>-1</sup>, 25 mNm<sup>-1</sup>, 30 mNm<sup>-1</sup> and 40 mNm<sup>-1</sup> of DPPC:POPG:PA before ozone exposure (top) and after ozone exposure (bottom).

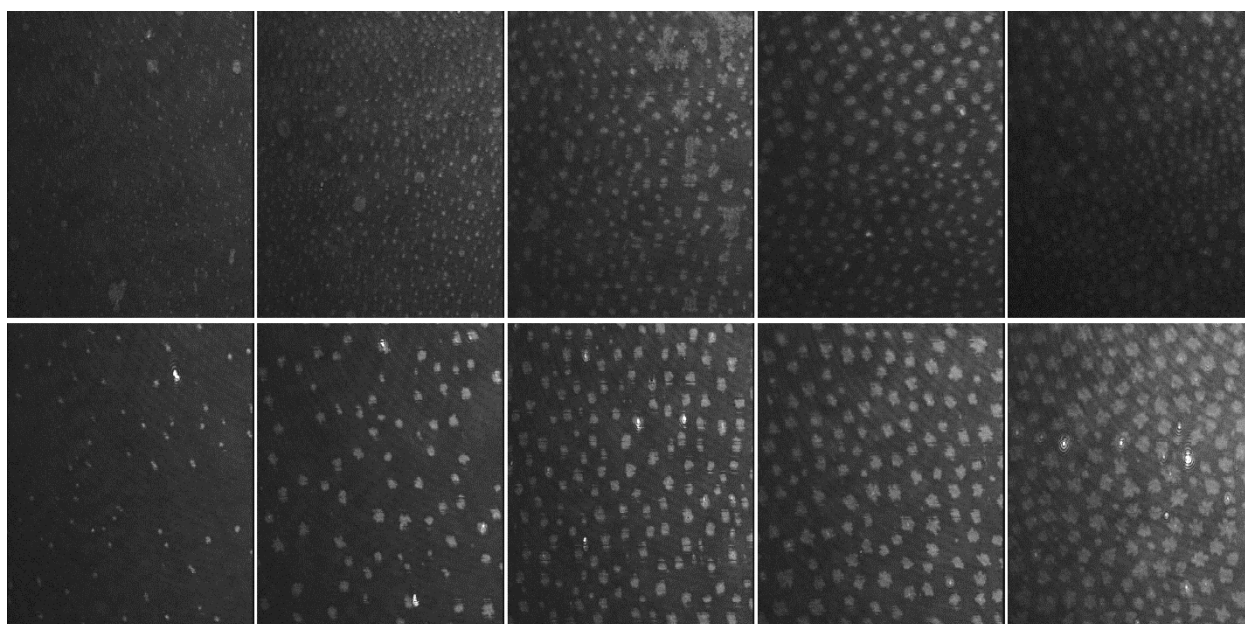


**Figure 3.4.** BAM images (220 nm width) of surface pressures (left to right): 10 mNm<sup>-1</sup>, 20 mNm<sup>-1</sup>, 25 mNm<sup>-1</sup>, 30 mNm<sup>-1</sup> and 40 mNm<sup>-1</sup> of Infasurf before ozone exposure (top) and after ozone exposure (bottom).

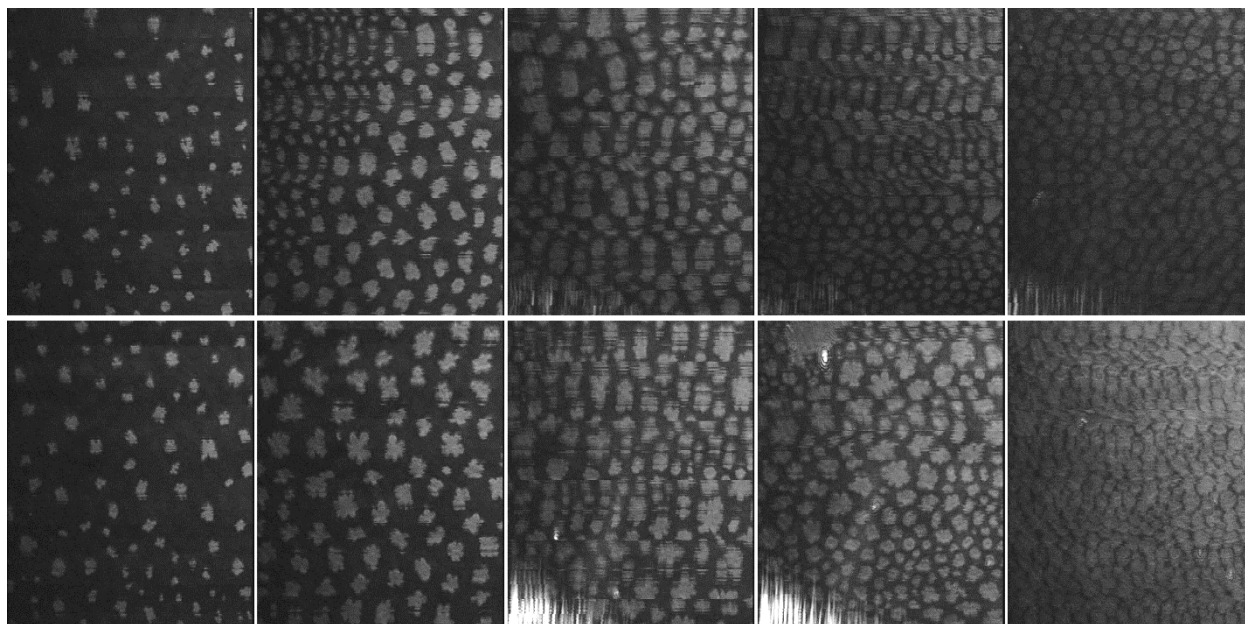


**Figure 3.5. BAM images (220 nm width) of surface pressures (left to right): 10 mNm<sup>-1</sup>, 20 mNm<sup>-1</sup>, 25 mNm<sup>-1</sup>, 30 mNm<sup>-1</sup> and 40 mNm<sup>-1</sup> of Survanta before ozone exposure (top) and after ozone exposure (bottom).**

The viscoelastic properties of the DPPC:POPG film (Fig. 3.6) before and after ozone exposure remain similar except between 10 and 15 mNm<sup>-1</sup> which coincides with the phase transition corresponding to the formation of the DPPC-rich condensed phase<sup>74, 81</sup>. The phase transition plateau is similarly much more pronounced before ozone exposure in the compression isotherm (Fig. 3.1). The lack of change in rheology and morphology despite a shift in the isotherm is likely because oxidation is taking place solely in the LE phase and the cleaved POPG chain is still surface active<sup>62</sup>. Moreover, there are no other components in this phase. Thus, the viscoelastic properties are governed more by the combination of a DPPC condensed phase surrounded by a liquid-expanded phase<sup>4</sup>. On the other hand, the viscoelastic properties of the other lipid-only system (Fig. 3.7), DPPC:POPG:PA, are evidently reduced after ozone exposure. Oxidation of the POPG may be causing redistribution of the PA which is present in both phases. As shown using grazing x-ray diffraction, the condensed phase is almost completely DPPC and PA, but, there also seems to be some incorporation of POPG in the presence of PA<sup>41</sup>.

In the case of the lipid-protein systems, both the compression isotherms and the morphology before and after ozone exposure exhibited little to no change except in squeeze-out pressure. Surprisingly, in terms of rheological parameters, both Infasurf and Survanta displayed an apparent decrease in viscoelasticity after ozone exposure (Fig. 3.8 & 3.9).

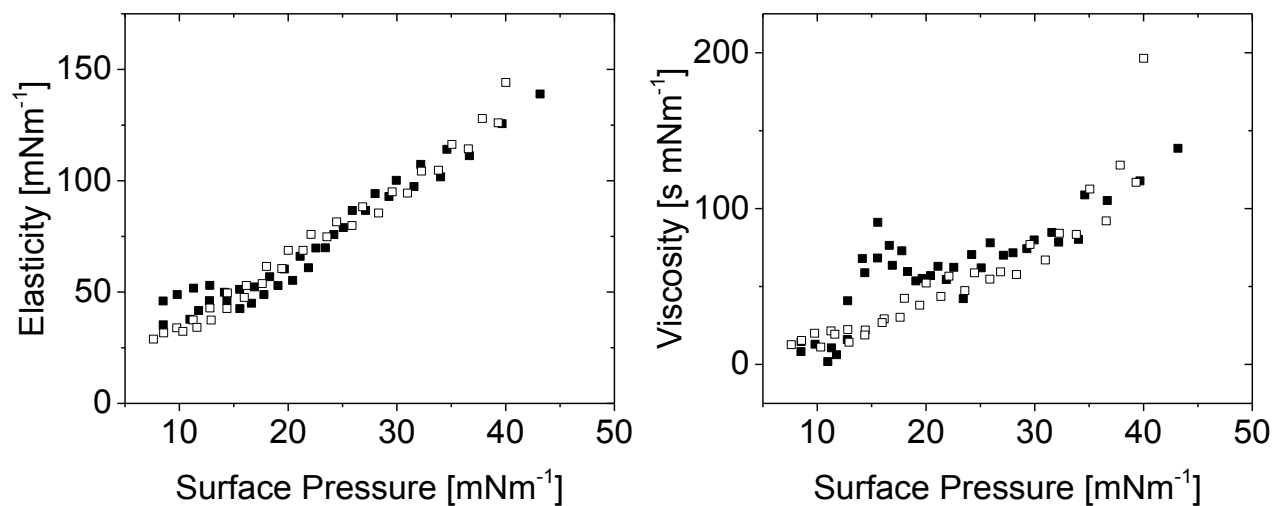


Figure 3.6. Surface dilational elasticity (left) and viscosity (right) data of DPPC:POPG before ozone exposure (■) and after ozone exposure (□).

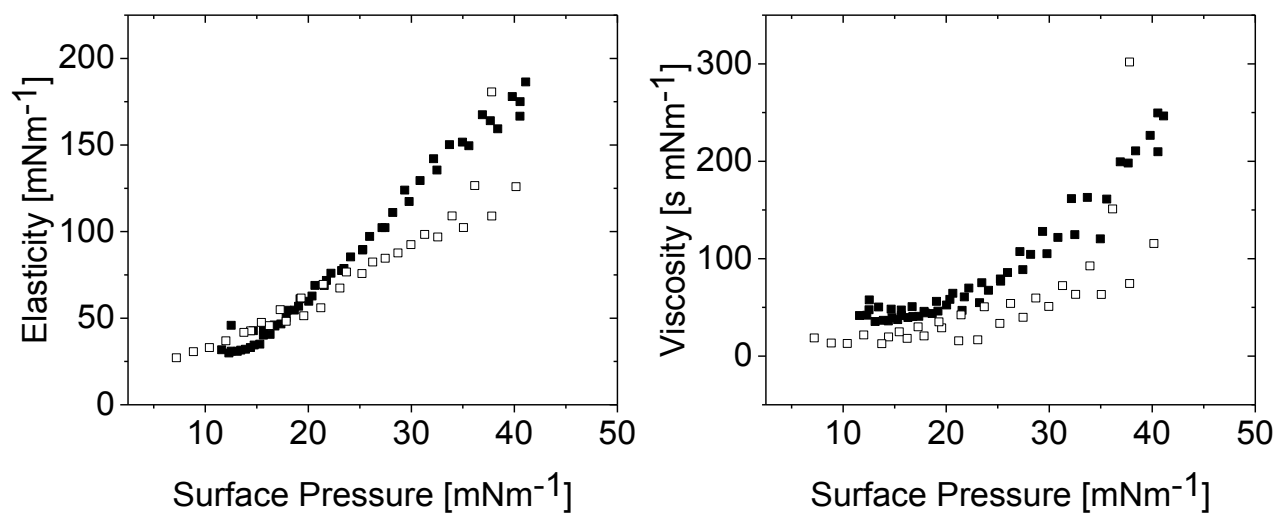
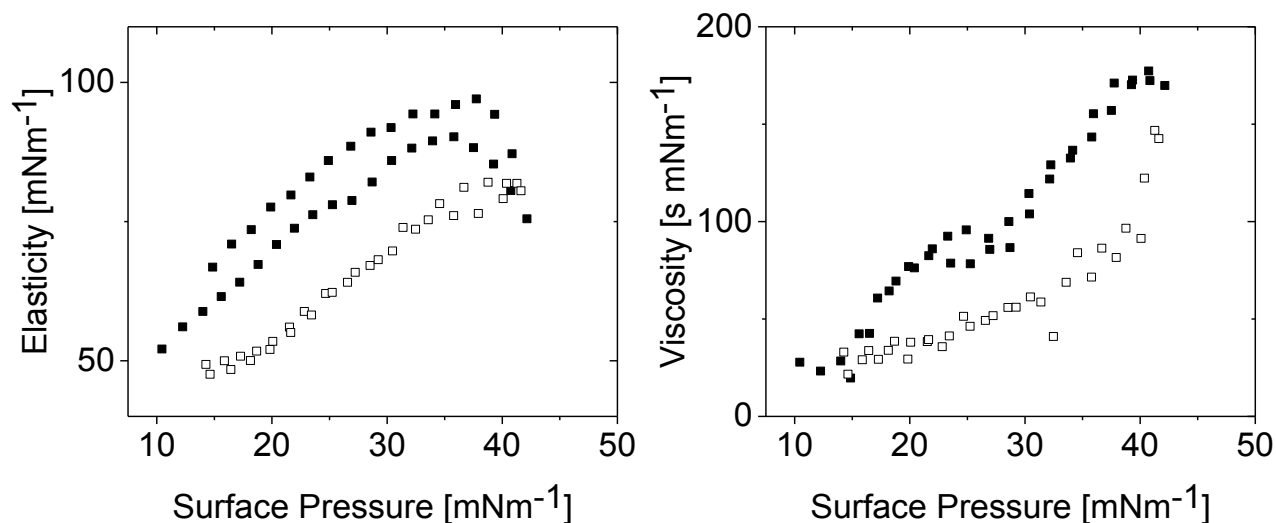
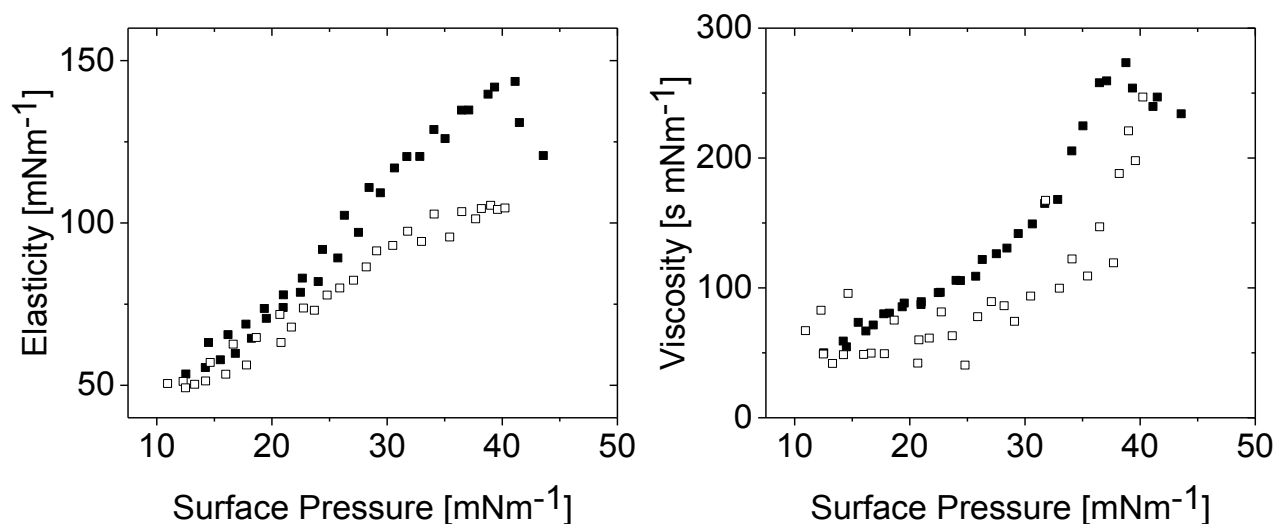


Figure 3.7. Surface dilational elasticity (left) and viscosity (right) data of DPPC:POPG:PA before ozone exposure (■) and after ozone exposure (□).



**Figure 3.8.** Surface dilational elasticity (left) and viscosity (right) data of Infasurf before ozone exposure (■) and after ozone exposure (□).



**Figure 3.9.** Surface dilational elasticity (left) and viscosity (right) data of Survanta before ozone exposure (■) and after ozone exposure (□).

Survanta is rich in SP-C but contains little SP-B. Oxidation of SP-C has resulted in reduced palmitoylation levels, where palmitoylation is important for reservoir formation. However, it is not yet clear whether the observed reduction in squeeze-out pressure is due to decreased palmitoylation or changes to amino acid residues<sup>82</sup>. Oxidation of Survanta films by environmental tobacco smoke resulted in increased area occupied by liquid expanded phase and in the appearance of fewer bilayer aggregates suggesting that there is less material retained at the surface after exposure<sup>43</sup>. This lack of material retention may be because of decreased palmitoylation of SP-C.

However, modification of SP-C by replacing the palmitoylated cysteines with phenylalanines did not seem to affect the monolayer<sup>7</sup>. The changes in the rheological parameters after ozone exposure in Survanta may be due to a combination of factors including oxidation of amino acids, decreases in palmitoylation of SP-C but also the added PA.

Infasurf, on the other hand, contains high amounts of SP-B in comparison to Survanta and alterations in the sequence of SP-B have been shown to affect film properties. For example modification of the N-terminal proline residues to alanines reduced the effectiveness of reinsertion of the surface material into the expanding film<sup>10</sup>. The reduced effectiveness of reinsertion indicates a reduced amount of material at the interface and therefore a reduction in rheological parameters. Ozone exposure may lead to oxidation of such residues and this may explain the decrease in rheology seen in Infasurf. SP-B has been shown to be oxidized by ozone at the air-water interface, where only the oxidizable residues exposed to the air are affected<sup>63</sup>. Further, oxidation of SP-B by reactive oxygen species produced by the Fenton reaction had shown a reduction in surface activity which may be due to a decrease in positively charged amino acids interacting with the lipid monolayer<sup>82</sup>.

After ozone exposure, the elasticity of Infasurf and Survanta (Appendix A, Fig. A10) is less than the elasticity of their counterpart model systems, DPPC:POPG and DPPC:POPG:PA respectively although the difference between Infasurf and DPPC:POPG is more pronounced than the difference between Survanta and DPPC:POPG:PA. This may be because of the high amounts of SP-B present in Infasurf which appears to have a more substantial role in the physicochemical parameters of LS than SP-C since, the addition of SP-B to oxidized SP-C films improves the surface activity but not vice-versa<sup>82</sup>. Moreover, SP-B deficiencies are known to be fatal, i.e. a compromised lung surfactant system, while SP-C deficiencies are less severe<sup>29</sup>. In order to easily compare, overlays of dilational elasticity and viscosity of all four systems before and after ozone exposure can be found in Appendix A. Before ozone exposure, however, the elasticity of DPPC:POPG and Infasurf and DPPC:POPG:PA and Survanta (Appendix A, Fig. A5) are quite similar until higher pressures. In terms of viscosity, all films exhibit similar viscosities after ozone exposure (Appendix A, Fig. A10), but Infasurf and Survanta exhibit greater viscosities than their counterparts, DPPC:POPG and DPPC:POPG:PA respectively, before ozone exposure (Appendix A, Fig. A5). The changes in viscoelasticity as a function of composition indicates that exposure to

ozone is affecting the proteins in the film directly and therefore it is affecting protein-lipid interactions.

Interestingly, the viscoelastic properties of both Survanta and Infasurf are not affected by ozone exposure when using water as the subphase (Appendix A, Fig. A13 & A14) whereas the lipid-only systems exhibit the same trend on either subphase (Appendix A, Fig. A11 & A12). Likely the buffer on the proteins either moderates their conformation and orientation at the interface in general which may either impact the general viscoelastic properties by modifying their ability to perform their physiological role or may induce different residues to be exposed at the surface and thus more susceptible to oxidation.

### 3.5. Conclusion

Exposure of all four systems to ozone leads to lowered squeeze-out pressures. However, only the compression isotherms of the lipid-only systems exhibited a shift to higher molecular area after exposure. This is attributed to accommodation of the cleaved POPG chain. The lipid-protein systems did not show such a shift which may be due to the presence of polyunsaturated lipids. DPPC:POPG is the only system that showed clear changes in BAM images, where early squeeze-out of the LE phase after exposure was observed. This is because of the increased solubility of POPG and the lack of surfactant proteins to maintain the LE phase at the interface. The DPPC:POPG:PA, Survanta and Infasurf systems did not display such a difference using BAM which we believe is because the squeeze-out pressure before and after ozone exposure was not reached when referring to the compression isotherm. In the case of Survanta and Infasurf, it may also be possible that the surfactant proteins are maintaining LE phase at the interface. The viscoelasticity of the DPPC:POPG film did not change after exposure but was reduced for all of the other systems. This could be because in the DPPC:POPG system, the cleaved POPG chain is still surface-active. The reduction in DPPC:POPG:PA may be due to redistribution of the PA phase after exposure. However, the rheology data for Infasurf and Survanta is more complicated to elucidate. The reduction after ozone exposure can be due to a number of factors: the presence of polyunsaturated lipids, the presence of surfactant proteins and in the case of Survanta, the presence of PA. The reduction in viscoelastic properties induced by ozone exposure may destabilize the LS film within our alveoli, since high surface viscosity with increasing surface pressure has been associated with stabilizing LS within the alveoli to prevent outward flow of LS due to the surface

tension gradient present in our lungs<sup>30</sup>. This work offers insight into the impact of ozone on model lung surfactant films. We show that ozone exposure does indeed reduce lung surfactant functioning.

## Chapter 4. Conclusions and Future Work

The purpose of this thesis research was to determine the impact of ozone exposure on model lung surfactant films as a function of composition. First the difference between using a water subphase versus a more physiologically relevant buffer was explored. The use of either water or buffer can be found in the literature and this inconsistency provided a potential source of error and needed to be understood and controlled to draw appropriate conclusions based on comparison to previous work. Therefore the first manuscript is devoted to probing the impact of added salt and buffer on the phase behaviour of model lung surfactant systems.

The water versus buffer analysis yielded several interesting results. Firstly, based on compression isotherms, all four model LS films were slightly more expanded on buffer than on water. This was attributed to the presence of the anionic POPG lipid, since the sodium cations can insert between the headgroups. Further, BAM imaging showed similar findings. However, in the case of Survanta, there did not appear to be much a difference, perhaps implying that of the two proteins, SP-C is not as affected by the presence of salt. In this regard, SP-C only has two charged amino acid residues while SP-B has seven. Rheology measurements exhibit an apparent reduction in viscoelastic parameters when salt is present for all systems except Infasurf. This reduction is explained by the film expansion, since a condensed phase reaches higher viscoelasticity values than a LE phase. However, for Infasurf this is not the case and this is attributed to the presence of high amounts of SP-B which is positively charged. For this reason, perhaps the lipid phases are not as affected with the addition salt: they already have a counterion in the form of the protein. Further investigation using GIXD measurements, again demonstrates a film expansion in all cases except Survanta which has a reduced tilt angle upon addition of salt. Since this data was taken from the literature and because Survanta is an animal extract, it is possible the variation is due to sample variability and the use of sodium bicarbonate instead of tris. For this reason, it is necessary to test Survanta using our own conditions (same extract batch, same buffer). Compositionally, the presence of palmitic acid always leads to higher viscoelasticities which is attributed to the improved packing that PA provides. However, the addition of salt does cause the rheology of the lipid-protein systems in comparison to the lipid-only systems to behave differently than on water. This outlines that the proteins are somehow being affected by the presence of salt and therefore the importance of studying the impact of salt on model LS films.

To probe for the effect of buffer on the lipid-protein systems even further, GIXD analysis should be done on systems containing cholesterol to look for the presence of a cholesterol phase to see if this is indeed what we saw at low  $Q_{xy}$  with Infasurf. Adding the cholesterol to the lipid-only system would improve the signal-to-noise for fitting purposes by reducing the amount of liquid-expanded phase and allow systematic variation of the amount of cholesterol to determine the critical amount required for formation of a liquid-ordered phase, which has been shown to improve the activity of bovine lipid extract surfactant. However when the amount of cholesterol exceeds the amount of saturated phospholipids it leads to the formation of a liquid-disordered phase which disrupts the activity of LS<sup>83</sup>. High levels of cholesterol in LS have been found in acutely injured lungs, where these lungs exhibit a decrease in lung compliance (a more rigid lung) associated with diseases such as pulmonary fibrosis<sup>84, 85</sup>. To study the effect of cholesterol even more, similar analyses regarding compression isotherms, BAM images and rheological data can be done to see the impact of buffer on cholesterol. Also, it would be necessary to take GIXD measurements of Survanta on both water and buffer so that the composition of film and subphase can be carefully controlled to see if the tilt angle decreases or increases going from water to buffer.

Once the effect of salt on model LS films was established, the impact of ozone exposure on such films could be studied on both water and buffer subphases. However, the data presented in this work is on buffer only where the data on water can be found in Appendix A. Compression isotherms of the lipid-only systems show shifts to higher molecular area after ozone exposure. This is due to the accommodation of the cleaved POPG chain. The lipid-protein systems do not exhibit such a shift which may be due to a compensatory effect enabled by the presence of polyunsaturated lipids as well as the surfactant proteins. BAM imaging displayed an early squeeze-out of the DPPC:POPG system after exposure, but not for the other three systems. This may be because the squeeze-out before and after ozone exposure was higher than  $40 \text{ mNm}^{-1}$  (highest pressure attainable on the Langmuir film balance used) or in the case of the lipid-protein systems, the proteins may be retaining the LE phase at the air-liquid interface. Further, rheology measurements indicate a decrease in viscoelasticity for all systems except DPPC:POPG. The lack of the reduction in viscoelasticity for DPPC:POPG may be because the cleaved POPG chain is still surface-active. For DPPC:POPG:PA, there may be a redistribution of PA between the phases occurring after exposure leading to the decrease in rheological properties since PA does improve the packing in the condensed phase. In the case of the lipid-protein systems, the reduction after exposure seen

with Infasurf could be due to the presence of polyunsaturated lipids but also because of the high amounts of SP-B present which is indeed affected by oxidation. Similarly, the reduction seen in Survanta could be because of the presence of the polyunsaturated lipids, surfactant proteins but also because of the PA present, since, DPPC:POPG:PA is highly affected by ozone exposure but DPPC:POPG is not. Interestingly, the rheology of the lipid-only systems behave similarly on water as on TBS after ozone exposure but the lipid-protein systems did not seem to be affected by ozone on water. This leads to the notion that the buffer may be inducing a change in protein orientation or structure, outlining, again the importance of studying the impact of buffer on LS. Compositionally, the most striking change after ozone exposure, is that viscosity for all systems reach similar values at all surface pressures on buffer. This indicates that ozone is indeed affecting the proteins and therefore the lipid-protein interactions.

To further pinpoint the change in rheology after ozone exposure of the lung surfactant replacement therapies, amino acid sequencing by mass spectrometry of oxidized and unoxidized films may offer insight into amino acid oxidation and therefore possible changes in protein structure and function. Initial attempts to perform ESI-MS on oxidized Infasurf and Survanta films were unsuccessful since the amount of protein in the films collected from the PAT were insufficient for analysis. This should be performed further by adapting the MS methods of Liu *et al*<sup>79</sup> and Kim *et al*<sup>63</sup>. Further, grazing incidence x-ray diffraction after ozone exposure of all films would give information about changes in monolayer structure and possible PA redistribution. Temperature dependence studies before and after exposure can also be done to make this work even more physiologically relevant although literature<sup>30</sup> has shown the phase behaviour to be similar. To follow changes in reservoir thickness, atomic force microscopy can be done before and after exposure. Finally, as mentioned before, studying the effect of the addition of cholesterol would lead to further understanding of the effect of composition. Future challenges also include studying the impact of different pollutants individually and in combination on LS including hydroxyl radicals, NO<sub>x</sub>, polycyclic aromatic hydrocarbons (PAHs) and particulate matter.

To generalize the findings of this thesis research, the presence of salt leads to expansion of LS films and exposure of these films to ozone leads to reduced LS functioning. The implication of these findings suggest that high ambient ground-level ozone concentrations are harmful to our health especially for people with compromised immune systems or that have a respiratory disease. However, this research may possibly lead to better insight on the effect of atmospheric pollutants

on the breathing cycle as well as improving lung surfactant replacement therapies to better treat respiratory ailments.

## Chapter 5. References

1. Schürch, S.; Goerke, J.; Clements, J. A., Direct determination of surface tension in the lung. *Proceedings of the National Academy of Sciences* **1976**, *73* (12), 4698-4702.
2. Bernardino de la Serna, J.; Perez-Gil, J.; Simonsen, A. C.; Bagatolli, L. A., Cholesterol rules: direct observation of the coexistence of two fluid phases in native pulmonary surfactant membranes at physiological temperatures. *The Journal of Biological Chemistry* **2004**, *279* (39), 40715-22.
3. Bringezu, F.; Ding, J.; Brezesinski, G.; Waring, A. J.; Zasadzinski, J. A., Influence of Pulmonary Surfactant Protein B on Model Lung Surfactant Monolayers. *Langmuir : The ACS Journal of Surfaces and Colloids* **2002**, *18* (6), 2319-2325.
4. Alonso, C.; Alig, T.; Yoon, J.; Bringezu, F.; Warriner, H.; Zasadzinski, J. A., More Than a Monolayer: Relating Lung Surfactant Structure and Mechanics to Composition. *Biophysical Journal* **2004**, *87* (6), 4188-4202.
5. Zasadzinski, J. A.; Ding, J.; Warriner, H. E.; Bringezu, F.; Waring, A. J., The physics and physiology of lung surfactants. *Current Opinion in Colloid & Interface Science* **2001**, *6* (5-6), 506-513.
6. Alonso, C.; Bringezu, F.; Brezesinski, G.; Waring, A. J.; Zasadzinski, J. A., Modifying Calf Lung Surfactant by Hexadecanol. *Langmuir : The ACS Journal of Surfaces and Colloids* **2005**, *21* (3), 1028-1035.
7. Ding, J.; Takamoto, D. Y.; von Nahmen, A.; Lipp, M. M.; Lee, K. Y. C.; Waring, A. J.; Zasadzinski, J. A., Effects of Lung Surfactant Proteins, SP-B and SP-C, and Palmitic Acid on Monolayer Stability. *Biophysical Journal* **2001**, *80* (5), 2262-2272.
8. Hawgood, S., Surfactant protein B: structure and function. *Biology of the Neonate* **2004**, *85* (4), 285-9.
9. Notter, R. H.; Wang, Z.; Egan, E. A.; Holm, B. A., Component-specific surface and physiological activity in bovine-derived lung surfactants. *Chemistry and Physics of Lipids* **2002**, *114* (1), 21-34.
10. Sharifahmadian, M.; Sarker, M.; Palleboina, D.; Waring, A. J.; Walther, F. J.; Morrow, M. R.; Booth, V., Role of the N-terminal seven residues of surfactant protein B (SP-B). *PLoS ONE* **2013**, *8* (9), e72821.

11. Zhang, H.; Fan, Q.; Wang, Y. E.; Neal, C. R.; Zuo, Y. Y., Comparative study of clinical pulmonary surfactants using atomic force microscopy. *Biochimica et Biophysica Acta (BBA) - Biomembranes* **2011**, *1808* (7), 1832-1842.
12. Veldhuizen, R.; Nag, K.; Orgeig, S.; Possmayer, F., The role of lipids in pulmonary surfactant. *Biochimica et Biophysica Acta (BBA) - Molecular Basis of Disease* **1998**, *1408* (2-3), 90-108.
13. Rüdiger, M.; Tölle, A.; Meier, W.; Rüstow, B., *Naturally derived commercial surfactants differ in composition of surfactant lipids and in surface viscosity*. 2005; Vol. 288, p L379-L383.
14. LeVine, A. M.; Whitsett, J. A.; Gwozdz, J. A.; Richardson, T. R.; Fisher, J. H.; Burhans, M. S.; Korfhagen, T. R., Distinct Effects of Surfactant Protein A or D Deficiency During Bacterial Infection on the Lung. *The Journal of Immunology* **2000**, *165* (7), 3934-3940.
15. Cockshutt, A. M.; Weitz, J.; Possmayer, F., Pulmonary surfactant-associated protein A enhances the surface activity of lipid extract surfactant and reverses inhibition by blood proteins in vitro. *Biochemistry* **1990**, *29* (36), 8424-8429.
16. Kishore, U.; Greenhough, T. J.; Waters, P.; Shrive, A. K.; Ghai, R.; Kamran, M. F.; Bernal, A. L.; Reid, K. B. M.; Madan, T.; Chakraborty, T., Surfactant proteins SP-A and SP-D: Structure, function and receptors. *Molecular Immunology* **2006**, *43* (9), 1293-1315.
17. Korfhagen, T. R.; Sheftelyevich, V.; Burhans, M. S.; Bruno, M. D.; Ross, G. F.; Wert, S. E.; Stahlman, M. T.; Jobe, A. H.; Ikegami, M.; Whitsett, J. A.; Fisher, J. H., Surfactant Protein-D Regulates Surfactant Phospholipid Homeostasis in Vivo. *Journal of Biological Chemistry* **1998**, *273* (43), 28438-28443.
18. Schurch, S.; Possmayer, F.; Cheng, S.; Cockshutt, A. M., *Pulmonary SP-A enhances adsorption and appears to induce surface sorting of lipid extract surfactant*. 1992; Vol. 263, p L210-L218.
19. Wright, J. R.; Borchelt, J. D.; Hawgood, S., Lung surfactant apoprotein SP-A (26-36 kDa) binds with high affinity to isolated alveolar type II cells. *Proceedings of the National Academy of Sciences* **1989**, *86* (14), 5410-5414.
20. Wright, J. R.; Wager, R. E.; Hawgood, S.; Dobbs, L.; Clements, J. A., Surfactant apoprotein Mr = 26,000-36,000 enhances uptake of liposomes by type II cells. *Journal of Biological Chemistry* **1987**, *262* (6), 2888-2894.

21. Hartshorn, K. L.; Crouch, E. C.; White, M. R.; Eggleton, P.; Tauber, A. I.; Chang, D.; Sastry, K., Evidence for a protective role of pulmonary surfactant protein D (SP-D) against influenza A viruses. *Journal of Clinical Investigation* **1994**, *94* (1), 311-319.
22. Kishore, U.; Madan, T.; Sarma, P. U.; Singh, M.; Urban, B. C.; Reid, K. B. M., Protective Roles of Pulmonary Surfactant Proteins, SP-A and SP-D, Against Lung Allergy and Infection Caused by *Aspergillus fumigatus*. *Immunobiology* **2002**, *205* (4–5), 610-618.
23. Schaub, B.; Westlake, R. M.; He, H.; Arestides, R.; Haley, K. J.; Campo, M.; Velasco, G.; Bellou, A.; Hawgood, S.; Poulain, F. R.; Perkins, D. L.; Finn, P. W., Surfactant protein D deficiency influences allergic immune responses. *Clinical & Experimental Allergy* **2004**, *34* (12), 1819-1826.
24. Hawgood, S.; Benson, B. J.; Schilling, J.; Damm, D.; Clements, J. A.; White, R. T., Nucleotide and amino acid sequences of pulmonary surfactant protein SP 18 and evidence for cooperation between SP 18 and SP 28-36 in surfactant lipid adsorption. *Proceedings of the National Academy of Sciences* **1987**, *84* (1), 66-70.
25. Veldhuizen, E. J. A.; Haagsman, H. P., Role of pulmonary surfactant components in surface film formation and dynamics. *Biochimica et Biophysica Acta (BBA) - Biomembranes* **2000**, *1467* (2), 255-270.
26. Johansson, J., Structure and properties of surfactant protein C. *Biochimica et Biophysica Acta (BBA) - Molecular Basis of Disease* **1998**, *1408* (2–3), 161-172.
27. Bringezu, F.; Pinkerton, K. E.; Zasadzinski, J. A., Environmental Tobacco Smoke Effects on the Primary Lipids of Lung Surfactant. *Langmuir : The ACS Journal of Surfaces and Colloids* **2003**, *19* (7), 2900-2907.
28. Schürch, S.; Green, F. H. Y.; Bachofen, H., Formation and structure of surface films: captive bubble surfactometry. *Biochimica et Biophysica Acta (BBA) - Molecular Basis of Disease* **1998**, *1408* (2–3), 180-202.
29. Wilder, M. A., Surfactant protein B deficiency in infants with respiratory failure. *The Journal of Perinatal & Neonatal Nursing* **2004**, *18* (1), 61-7.
30. Alonso, C.; Waring, A.; Zasadzinski, J. A., Keeping Lung Surfactant Where It Belongs: Protein Regulation of Two-Dimensional Viscosity. *Biophysical Journal* **2005**, *89* (1), 266-273.
31. Curstedt, T.; Johansson, J.; Persson, P.; Eklund, A.; Robertson, B.; Löwenadler, B.; Jörnvall, H., Hydrophobic surfactant-associated polypeptides: SP-C is a lipopeptide with two

palmitoylated cysteine residues, whereas SP-B lacks covalently linked fatty acyl groups. *Proceedings of the National Academy of Sciences* **1990**, *87* (8), 2985-2989.

32. Kim, K.; Choi, S. Q.; Zasadzinski, J. A.; Squires, T. M., Interfacial microrheology of DPPC monolayers at the air-water interface. *Soft Matter* **2011**, *7* (17), 7782-7789.

33. Grigoriev, D. O.; Krägel, J.; Akentiev, A. V.; Noskov, B. A.; Miller, R.; Pison, U., Relation between rheological properties and structural changes in monolayers of model lung surfactant under compression. *Biophysical Chemistry* **2003**, *104* (3), 633-642.

34. Wustneck, R.; Enders, P.; Wustneck, N.; Pison, U.; Miller, R.; Vollhardt, D., Surface dilational behaviour of spread dipalmitoyl phosphatidyl glycerol monolayers. *PhysChemComm* **1999**, *2* (11), 50-61.

35. Wüstneck, N.; Wüstneck, R.; Fainerman, V. B.; Miller, R.; Pison, U., Interfacial behaviour and mechanical properties of spread lung surfactant protein/lipid layers. *Colloids and Surfaces B: Biointerfaces* **2001**, *21* (1-3), 191-205.

36. Panaiotov, I.; Ivanova, T.; Proust, J.; Boury, F.; Denizot, B.; Keough, K.; Taneva, S., Effect of hydrophobic protein SP-C on structure and dilatational properties of the model monolayers of pulmonary surfactant. *Colloids and Surfaces B: Biointerfaces* **1996**, *6* (4-5), 243-260.

37. Stevens, T. P.; Sinkin, R. A., Surfactant replacement therapy. *Chest* **2007**, *131* (5), 1577-1582.

38. Tausch, H. W.; Lu, K.; Ramirez-Schrempp, D., Improving pulmonary surfactants. *Acta Pharmacologica Sinica* **2002**, *23* (SUPP), 11-15.

39. Ramanathan, R.; Rasmussen, M. R.; Gerstmann, D. R.; Finer, N.; Sekar, K.; The North American Study, G., A Randomized, Multicenter Masked Comparison Trial of Poractant Alfa (Curosurf) versus Beractant (Survanta) in the Treatment of Respiratory Distress Syndrome in Preterm Infants. *American Journal of Perinatology* **2004**, *21* (03), 109-119.

40. Bloom, B. T.; Kattwinkel, J.; Hall, R. T.; Delmore, P. M.; Egan, E. A.; Trout, J. R.; Malloy, M. H.; Brown, D. R.; Holzman, I. R.; Coghill, C. H.; Carlo, W. A.; Pramanik, A. K.; McCaffree, M. A.; Toubas, P. L.; Laudert, S.; Gratny, L. L.; Weatherstone, K. B.; Seguin, J. H.; Willett, L. D.; Gutcher, G. R.; Mueller, D. H.; Topper, W. H., Comparison of Infasurf (Calf Lung Surfactant Extract) to Survanta (Beractant) in the Treatment and Prevention of Respiratory Distress Syndrome. *Pediatrics* **1997**, *100* (1), 31-38.

41. Bringezu, F.; Ding, J.; Brezesinski, G.; Zasadzinski, J. A., Changes in Model Lung Surfactant Monolayers Induced by Palmitic Acid. *Langmuir : The ACS Journal of Surfaces and Colloids* **2001**, *17* (15), 4641-4648.
42. Stenger, P. C.; Wu, G.; Miller, C. E.; Chi, E. Y.; Frey, S. L.; Lee, K. Y. C.; Majewski, J.; Kjaer, K.; Zasadzinski, J. A., X-Ray Diffraction and Reflectivity Validation of the Depletion Attraction in the Competitive Adsorption of Lung Surfactant and Albumin. *Biophysical Journal* **2009**, *97* (3), 777-786.
43. Stenger, P. C.; Alonso, C.; Zasadzinski, J. A.; Waring, A. J.; Jung, C.-L.; Pinkerton, K. E., Environmental tobacco smoke effects on lung surfactant film organization. *Biochimica et Biophysica Acta (BBA) - Biomembranes* **2009**, *1788* (2), 358-370.
44. Bakshi, M. S.; Zhao, L.; Smith, R.; Possmayer, F.; Petersen, N. O., Metal Nanoparticle Pollutants Interfere with Pulmonary Surfactant Function In Vitro. *Biophysical Journal* **2008**, *94* (3), 855-868.
45. Leo, B. F.; Chen, S.; Kyo, Y.; Herpoldt, K. L.; Terrill, N. J.; Dunlop, I. E.; McPhail, D. S.; Shaffer, M. S.; Schwander, S.; Gow, A.; Zhang, J.; Chung, K. F.; Tetley, T. D.; Porter, A. E.; Ryan, M. P., The stability of silver nanoparticles in a model of pulmonary surfactant. *Environmental Science & Technology* **2013**, *47* (19), 11232-40.
46. Guzmán, E.; Liggieri, L.; Santini, E.; Ferrari, M.; Ravera, F., Influence of silica nanoparticles on phase behavior and structural properties of DPPC—Palmitic acid Langmuir monolayers. *Colloids and Surfaces A: Physicochemical and Engineering Aspects* **2012**, *413*, 280-287.
47. Guzmán, E.; Liggieri, L.; Santini, E.; Ferrari, M.; Ravera, F., Influence of silica nanoparticles on dilational rheology of DPPC—palmitic acid Langmuir monolayers. *Soft Matter* **2012**, *8* (14), 3938.
48. Finlayson-Pitts, B. J.; Pitts, J. N., Tropospheric Air Pollution: Ozone, Airborne Toxics, Polycyclic Aromatic Hydrocarbons, and Particles. *Science* **1997**, *276* (5315), 1045-1051.
49. Crutzen, P. J., Introductory lecture. Overview of tropospheric chemistry: developments during the past quarter century and a look ahead. *Faraday Discussions* **1995**, *100* (0), 1-21.
50. Jacob, D. J., Heterogeneous chemistry and tropospheric ozone. *Atmospheric Environment* **2000**, *34* (12–14), 2131-2159.

51. Hough, A. M.; Derwent, R. G., Changes in the global concentration of tropospheric ozone due to human activities. *Nature* **1990**, *344* (6267), 645-648.
52. Holton, J. R.; Haynes, P. H.; McIntyre, M. E.; Douglass, A. R.; Rood, R. B.; Pfister, L., Stratosphere-troposphere exchange. *Reviews of Geophysics* **1995**, *33* (4), 403-439.
53. Oltmans, S. J.; Lefohn, A. S.; Harris, J. M.; Galbally, I.; Scheel, H. E.; Bodeker, G.; Brunke, E.; Claude, H.; Tarasick, D.; Johnson, B. J.; Simmonds, P.; Shadwick, D.; Anlauf, K.; Hayden, K.; Schmidlin, F.; Fujimoto, T.; Akagi, K.; Meyer, C.; Nichol, S.; Davies, J.; Redondas, A.; Cuevas, E., Long-term changes in tropospheric ozone. *Atmospheric Environment* **2006**, *40* (17), 3156-3173.
54. Haagen-Smit, A. J., Chemistry and Physiology of Los Angeles Smog. *Industrial & Engineering Chemistry* **1952**, *44* (6), 1342-1346.
55. Basha, M. A.; Gross, K. B.; Gwizdala, C. J.; Haidar, A. H.; Popovich, J. J., BRonchoalveolar lavage neutrophilia in asthmatic and healthy volunteers after controlled exposure to ozone and filtered purified air. *Chest* **1994**, *106* (6), 1757-1765.
56. Tager, I. B.; Balmes, J.; Lurmann, F.; Ngo, L.; Alcorn, S.; Künzli, N., Chronic Exposure to Ambient Ozone and Lung Function in Young Adults. *Epidemiology* **2005**, *16* (6), 751-759.
57. Künzli, N.; Lurmann, F.; Segal, M.; Ngo, L.; Balmes, J.; Tager, I. B., Association between Lifetime Ambient Ozone Exposure and Pulmonary Function in College Freshmen—Results of a Pilot Study. *Environmental Research* **1997**, *72* (1), 8-23.
58. Jerrett, M.; Burnett, R. T.; Pope, C. A.; Ito, K.; Thurston, G.; Krewski, D.; Shi, Y.; Calle, E.; Thun, M., Long-Term Ozone Exposure and Mortality. *New England Journal of Medicine* **2009**, *360* (11), 1085-1095.
59. Pichavant, M.; Goya, S.; Meyer, E. H.; Johnston, R. A.; Kim, H. Y.; Matangkasombut, P.; Zhu, M.; Iwakura, Y.; Savage, P. B.; DeKruyff, R. H.; Shore, S. A.; Umetsu, D. T., Ozone exposure in a mouse model induces airway hyperreactivity that requires the presence of natural killer T cells and IL-17. *The Journal of Experimental Medicine* **2008**, *205* (2), 385-393.
60. Kim, H. I.; Kim, H.; Shin, Y. S.; Beegle, L. W.; Goddard, W. A.; Heath, J. R.; Kanik, I.; Beauchamp, J. L., Time Resolved Studies of Interfacial Reactions of Ozone with Pulmonary Phospholipid Surfactants Using Field Induced Droplet Ionization Mass Spectrometry. *The Journal of Physical Chemistry B* **2010**, *114* (29), 9496-9503.

61. Criegee, R., Mechanism of Ozonolysis. *Angewandte Chemie International Edition in English* **1975**, *14* (11), 745-752.
62. Thompson, K. C.; Jones, S. H.; Rennie, A. R.; King, M. D.; Ward, A. D.; Hughes, B. R.; Lucas, C. O.; Campbell, R. A.; Hughes, A. V., Degradation and rearrangement of a lung surfactant lipid at the air-water interface during exposure to the pollutant gas ozone. *Langmuir : The ACS Journal of Surfaces and Colloids* **2013**, *29* (14), 4594-602.
63. Kim, H. I.; Kim, H.; Shin, Y. S.; Beegle, L. W.; Jang, S. S.; Neidholdt, E. L.; Goddard, W. A.; Heath, J. R.; Kanik, I.; Beauchamp, J. L., Interfacial Reactions of Ozone with Surfactant Protein B in a Model Lung Surfactant System. *Journal of the American Chemical Society* **2010**, *132* (7), 2254-2263.
64. Grigoriev, D.; Krustev, R.; Miller, R.; Pison, U., Effect of Monovalent Ions on the Monolayers Phase Behavior of the Charged Lipid DPPG. *The Journal of Physical Chemistry B* **1999**, *103* (6), 1013-1018.
65. Zhao, W.; Róg, T.; Gurtovenko, A. A.; Vattulainen, I.; Karttunen, M., Atomic-Scale Structure and Electrostatics of Anionic Palmitoyloleoylphosphatidylglycerol Lipid Bilayers with Na<sup>+</sup> Counterions. *Biophysical Journal* **2007**, *92* (4), 1114-1124.
66. Garidel, P.; Blume, A., 1,2-Dimyristoyl-sn-glycero-3-phosphoglycerol (DMPG) monolayers: influence of temperature, pH, ionic strength and binding of alkaline earth cations. *Chemistry and Physics of Lipids* **2005**, *138* (1–2), 50-59.
67. Huang, Z.; Hua, W.; Verreault, D.; Allen, H. C., Influence of salt purity on Na<sup>+</sup> and palmitic acid interactions. *The Journal of Physical Chemistry A* **2013**, *117* (50), 13412-8.
68. Gurtovenko, A. A.; Vattulainen, I., Effect of NaCl and KCl on Phosphatidylcholine and Phosphatidylethanolamine Lipid Membranes: Insight from Atomic-Scale Simulations for Understanding Salt-Induced Effects in the Plasma Membrane. *The Journal of Physical Chemistry B* **2008**, *112* (7), 1953-1962.
69. Aroti, A.; Leontidis, E.; Maltseva, E.; Brezesinski, G., Effects of Hofmeister Anions on DPPC Langmuir Monolayers at the Air–Water Interface. *The Journal of Physical Chemistry B* **2004**, *108* (39), 15238-15245.
70. Tang, C. Y.; Allen, H. C., Ionic Binding of Na<sup>+</sup> versus K<sup>+</sup> to the Carboxylic Acid Headgroup of Palmitic Acid Monolayers Studied by Vibrational Sum Frequency Generation Spectroscopy†. *The Journal of Physical Chemistry A* **2009**, *113* (26), 7383-7393.

71. Mao, Y.; Du, Y.; Cang, X.; Wang, J.; Chen, Z.; Yang, H.; Jiang, H., Binding competition to the POPG lipid bilayer of  $\text{Ca}^{2+}$ ,  $\text{Mg}^{2+}$ ,  $\text{Na}^+$ , and  $\text{K}^+$  in different ion mixtures and biological implication. *The Journal of Physical Chemistry B* **2013**, *117* (3), 850-8.
72. Leser, M. E.; Acquistapace, S.; Cagna, A.; Makievski, A. V.; Miller, R., Limits of oscillation frequencies in drop and bubble shape tensiometry. *Colloids and Surfaces A: Physicochemical and Engineering Aspects* **2005**, *261* (1–3), 25-28.
73. Li, J. B.; Miller, R.; Vollhardt, D.; Weidemann, G.; Möhwald, H., Isotherms of phospholipid monolayers measured by a pendant drop technique. *Colloid and Polymer Science* **1996**, *274* (10), 995-999.
74. Vrânceanu, M.; Winkler, K.; Nirschl, H.; Leneweit, G., Surface rheology of monolayers of phospholipids and cholesterol measured with axisymmetric drop shape analysis. *Colloids and Surfaces A: Physicochemical and Engineering Aspects* **2007**, *311* (1–3), 140-153.
75. Stenger, P. C.; Wu, G.; Miller, C. E.; Chi, E. Y.; Frey, S. L.; Lee, K. Y.; Majewski, J.; Kjaer, K.; Zasadzinski, J. A., X-ray diffraction and reflectivity validation of the depletion attraction in the competitive adsorption of lung surfactant and albumin. *Biophysical Journal* **2009**, *97* (3), 777-86.
76. Vingarzan, R., A review of surface ozone background levels and trends. *Atmospheric Environment* **2004**, *38* (21), 3431-3442.
77. Gomez, A. L.; Lewis, T. L.; Wilkinson, S. A.; Nizkorodov, S. A., Stoichiometry of Ozonation of Environmentally Relevant Olefins in Saturated Hydrocarbon Solvents. *Environmental Science & Technology* **2008**, *42* (10), 3582-3587.
78. Cataldo, F., On the action of ozone on proteins. *Polymer Degradation and Stability* **2003**, *82* (1), 105-114.
79. Liu, S.; Zhao, L.; Manzanares, D.; Doherty-Kirby, A.; Zhang, C.; Possmayer, F.; Lajoie, G. A., Characterization of bovine surfactant proteins B and C by electrospray ionization mass spectrometry. *Rapid Communications in Mass Spectrometry* **2008**, *22* (2), 197-203.
80. Gonzalez-Labrada, E.; Schmidt, R.; DeWolf, C. E., Kinetic analysis of the ozone processing of an unsaturated organic monolayer as a model of an aerosol surface. *Physical Chemistry Chemical Physics* **2007**, *9* (43), 5814-5821.
81. Albrecht, O.; Gruler, H.; Sackmann, E., Pressure-composition phase diagrams of cholesterol/lecithin, cholesterol/phosphatidic acid, and lecithin/phosphatidic acid mixed

monolayers: A Langmuir film balance study. *Journal of Colloid and Interface Science* **1981**, *79* (2), 319-338.

82. Rodríguez-Capote, K.; Manzanares, D.; Haines, T.; Possmayer, F., Reactive Oxygen Species Inactivation of Surfactant Involves Structural and Functional Alterations to Surfactant Proteins SP-B and SP-C. *Biophysical Journal* **2006**, *90* (8), 2808-2821.

83. Keating, E.; Rahman, L.; Francis, J.; Petersen, A.; Possmayer, F.; Veldhuizen, R.; Petersen, N. O., Effect of Cholesterol on the Biophysical and Physiological Properties of a Clinical Pulmonary Surfactant. *Biophysical Journal* **2007**, *93* (4), 1391-1401.

84. Leonenko, Z.; Finot, E.; Vassiliev, V.; Amrein, M., Effect of cholesterol on the physical properties of pulmonary surfactant films: Atomic force measurements study. *Ultramicroscopy* **2006**, *106* (8–9), 687-694.

85. Jankowich, M. D.; Rounds, S. I. S., Combined Pulmonary Fibrosis and Emphysema Syndrome: A Review. *Chest* **2012**, *141* (1), 222-231.

## Appendix A

Figures A1 and A2 are briefly described in section 2.4 and show the comparison for using TBS and PBS as the subphase, where there is minimal difference in terms of compression isotherms. However, the use of either buffer exhibits an expansion of the lipid-only films.

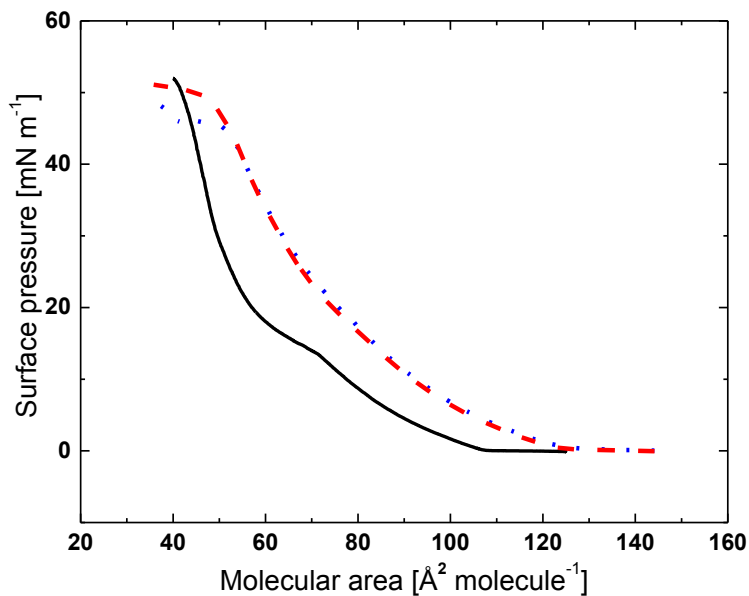


Figure A1. Compression isotherms of DPPC:POPG on water (—), TBS (---) and PBS (-·-).

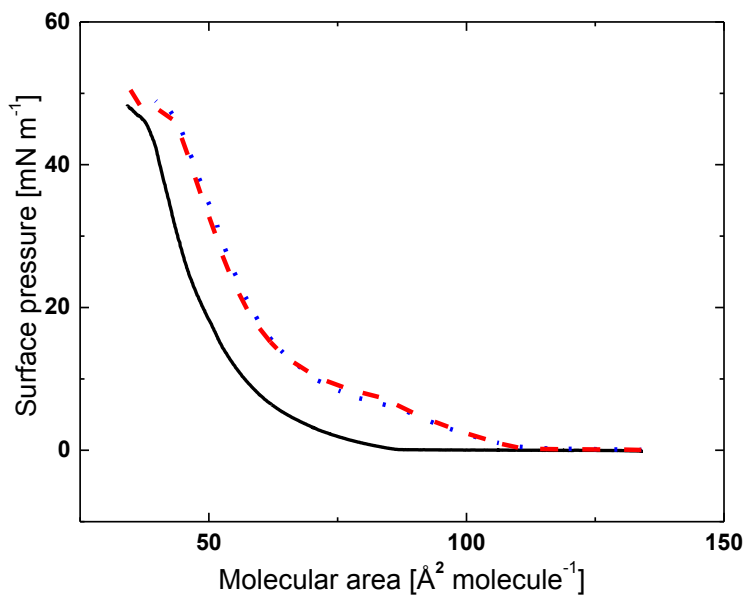
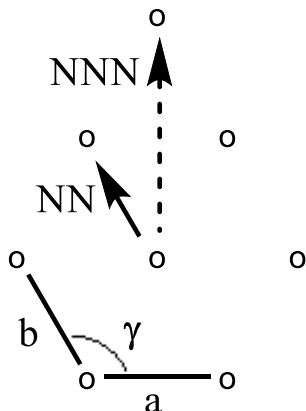


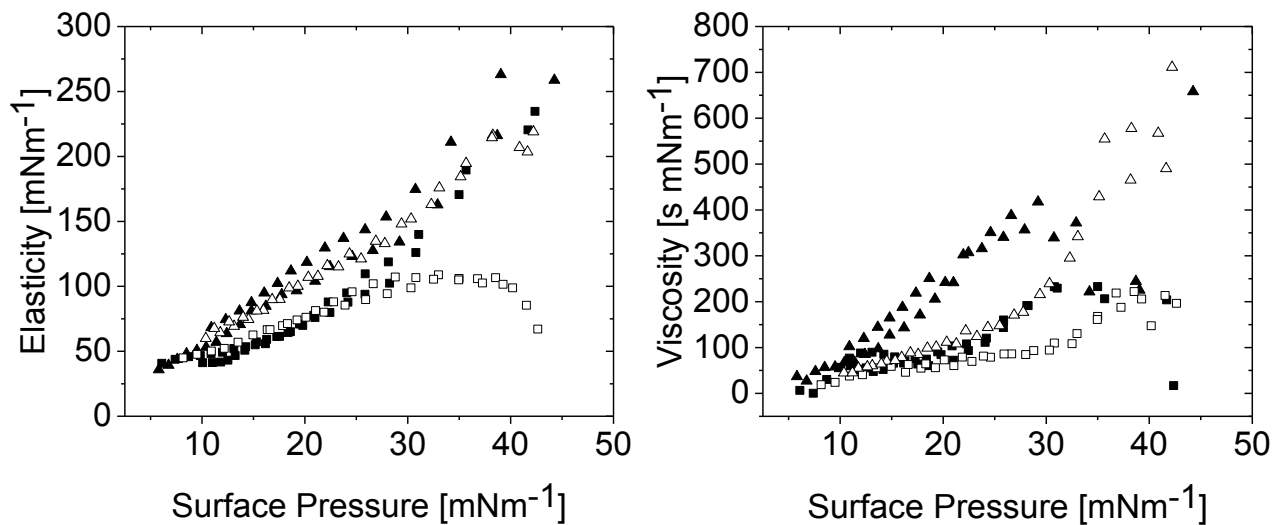
Figure A2. Compression isotherms of DPPC:POPG:PA on water (—), TBS (---) and PBS (-·-).

Figure A3 supplements the GIXD analysis described in section 2.4 and defines the lipid unit cell parameters  $a$ ,  $b$  and  $\gamma$  and the tilt directions.



**Figure A3. Schematic depiction of the unit cell where each circle represents the position of the lipid in the plane of the interface, arrows show direction of the alkyl chain tilt towards either NN or NNN.**

Figures A4 and A5 are also briefly described in section 2.4. These figures overlay rheological data of all four model LS systems used on water and on buffer, respectively. Although the data is a repetition of the data presented earlier in chapter 2, this representation is provided for easier comparison of the changes in viscoelasticity associated with LS composition. The set of figures can then also be compared to see the impact of buffer and composition on rheology.



**Figure A4. Surface dilational elasticity and viscosity of DPPC:POPG (■), DPPC:POPG:PA (▲), Infasurf (□) and Survanta (△) on water.**

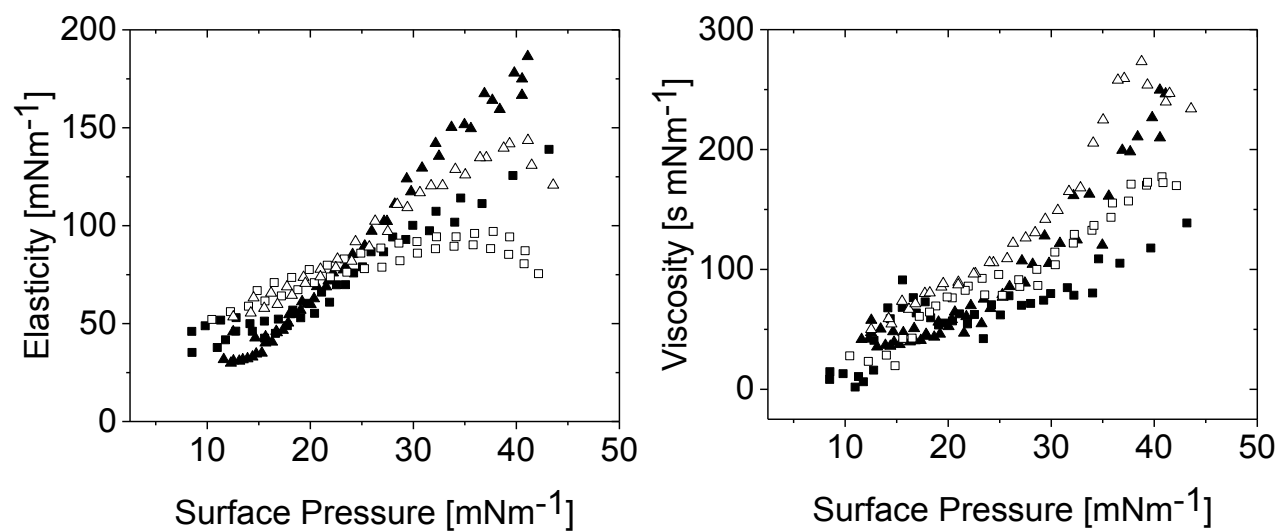


**Figure A5.** Surface dilational elasticity and viscosity of DPPC:POPG (■), DPPC:POPG:PA (▲), Infasurf (□) and Survanta (△) on TBS.

Figures A6 to A9 are mass spectra of the lipid-only systems before (A6 & A8) and after (A7 & A9) ozone exposure on water. Figures A8 & A9 were discussed briefly in section 3.4. These spectra show that POPG is oxidized upon exposure to ozone and that PA is not preventing the oxidation from occurring.

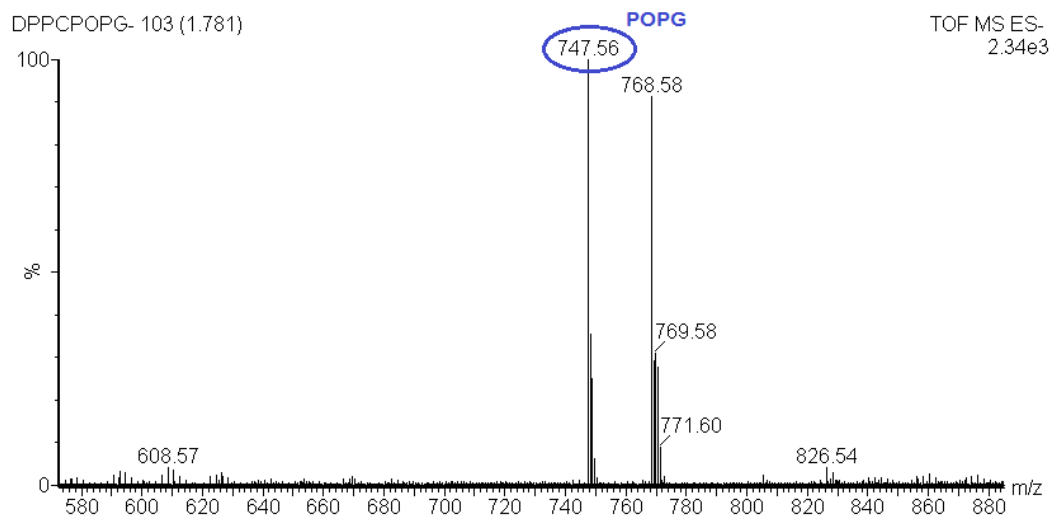


**Figure A6. Mass spectrum of DPPC:POPG before ozone exposure using ESI-MS.**

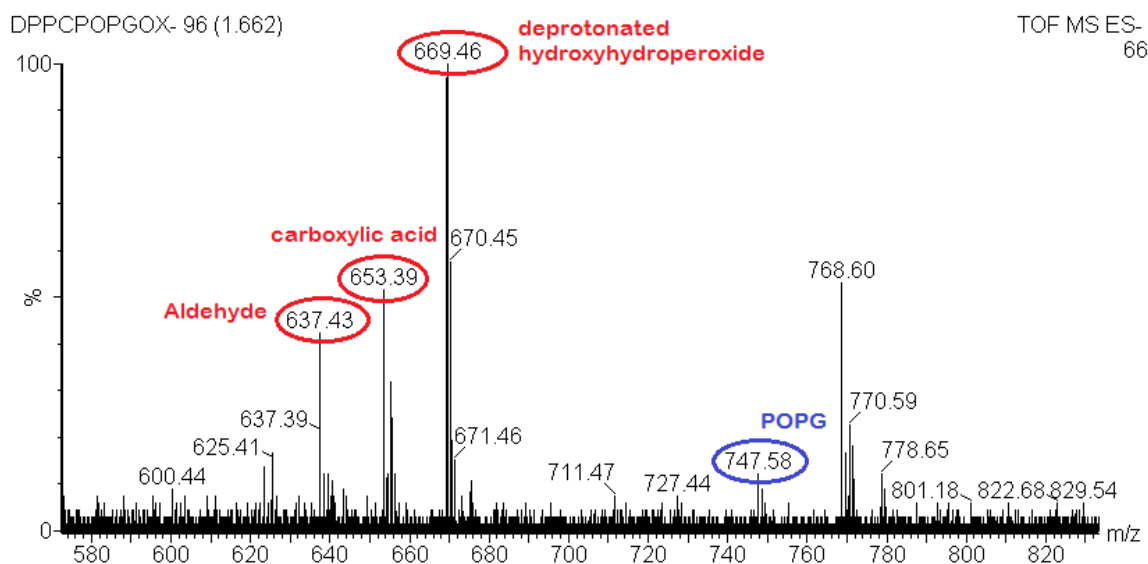


**Figure A7. Mass spectrum of DPPC:POPG after ozone exposure using ESI-MS.**

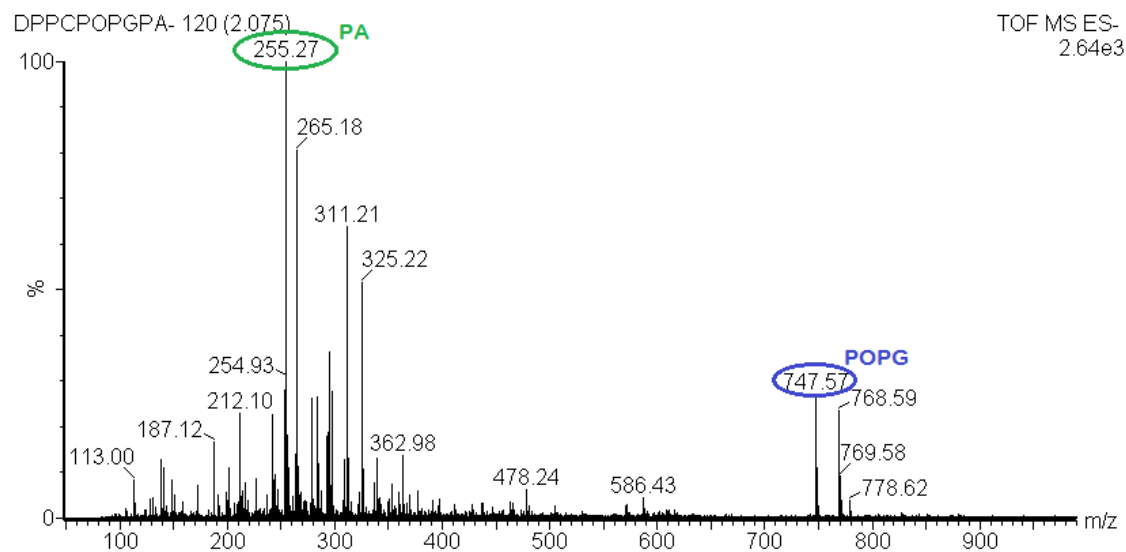


**Figure A8. Mass spectrum of DPPC:POPG:PA before ozone exposure using ESI-MS.**

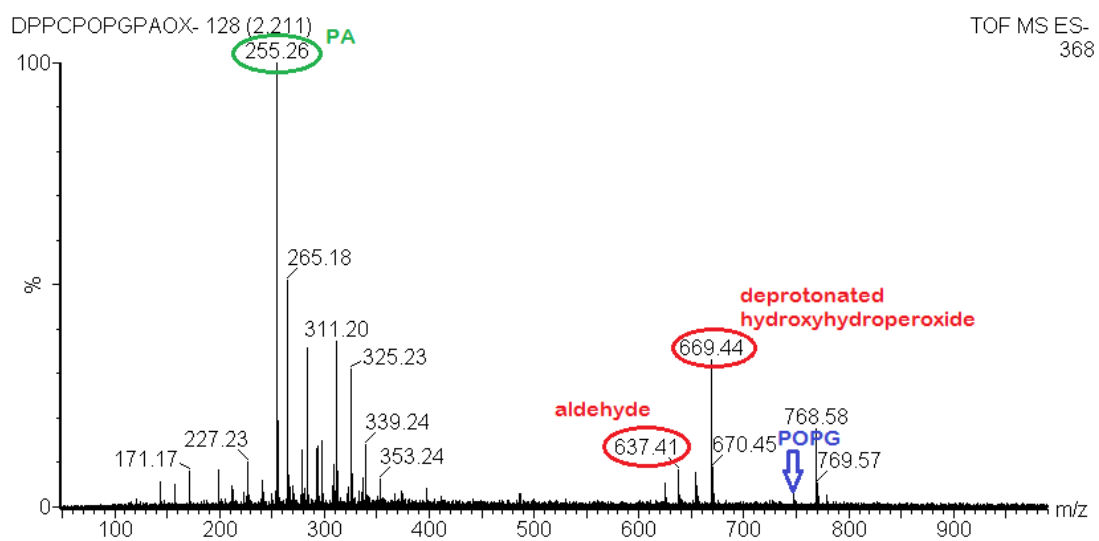


**Figure A9. Mass spectrum of DPPC:POPG:PA after ozone exposure using ESI-MS.**

Figure A10 was discussed in section 3.4 where it was also compared to Figure A5. Figure A10 shows the changes in rheological parameters after ozone exposure on TBS and allows us to determine the changes in viscoelasticity associated with LS composition. However, by comparing Figure A5 with Figure A10, all four systems before and after ozone exposure can be compared based on composition to determine the LS components which are affected more greatly by ozone exposure.

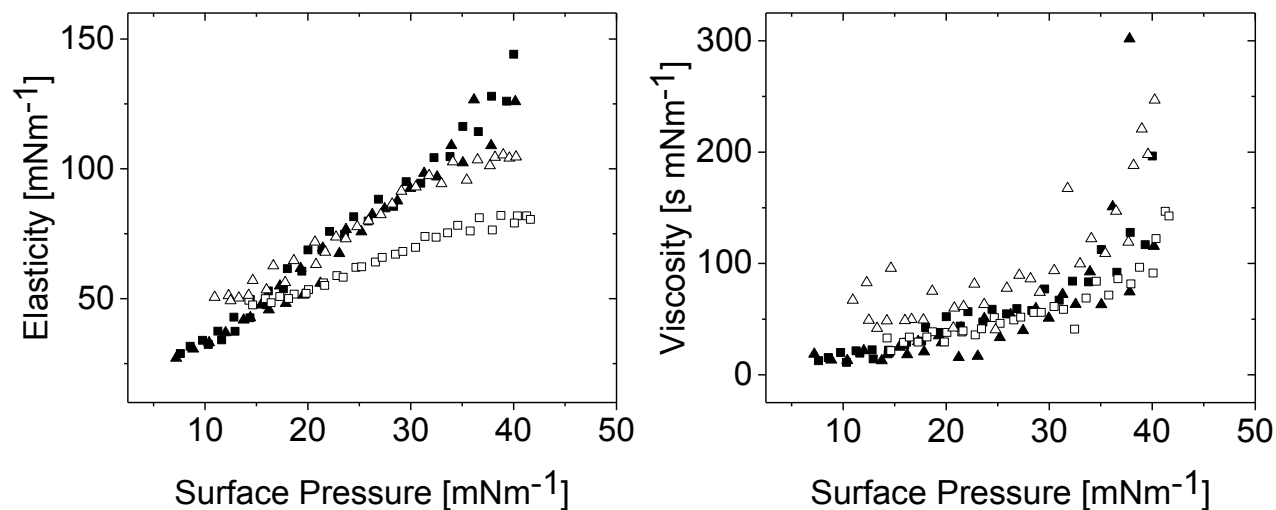


**Figure A10.** Surface dilational elasticity and viscosity of DPPC:POPG (■), DPPC:POPG:PA (▲), Infasurf (□) and Survanta (△) on TBS after ozone exposure.

Figures A11 to A16 are not discussed in the thesis. These figures are compression isotherms (A11) and rheological data (A12 – A16) of the four model LS systems before and after ozone exposure on water instead of TBS. These are presented here to show the difference in the biophysical impact of ozone based on a change in subphase.

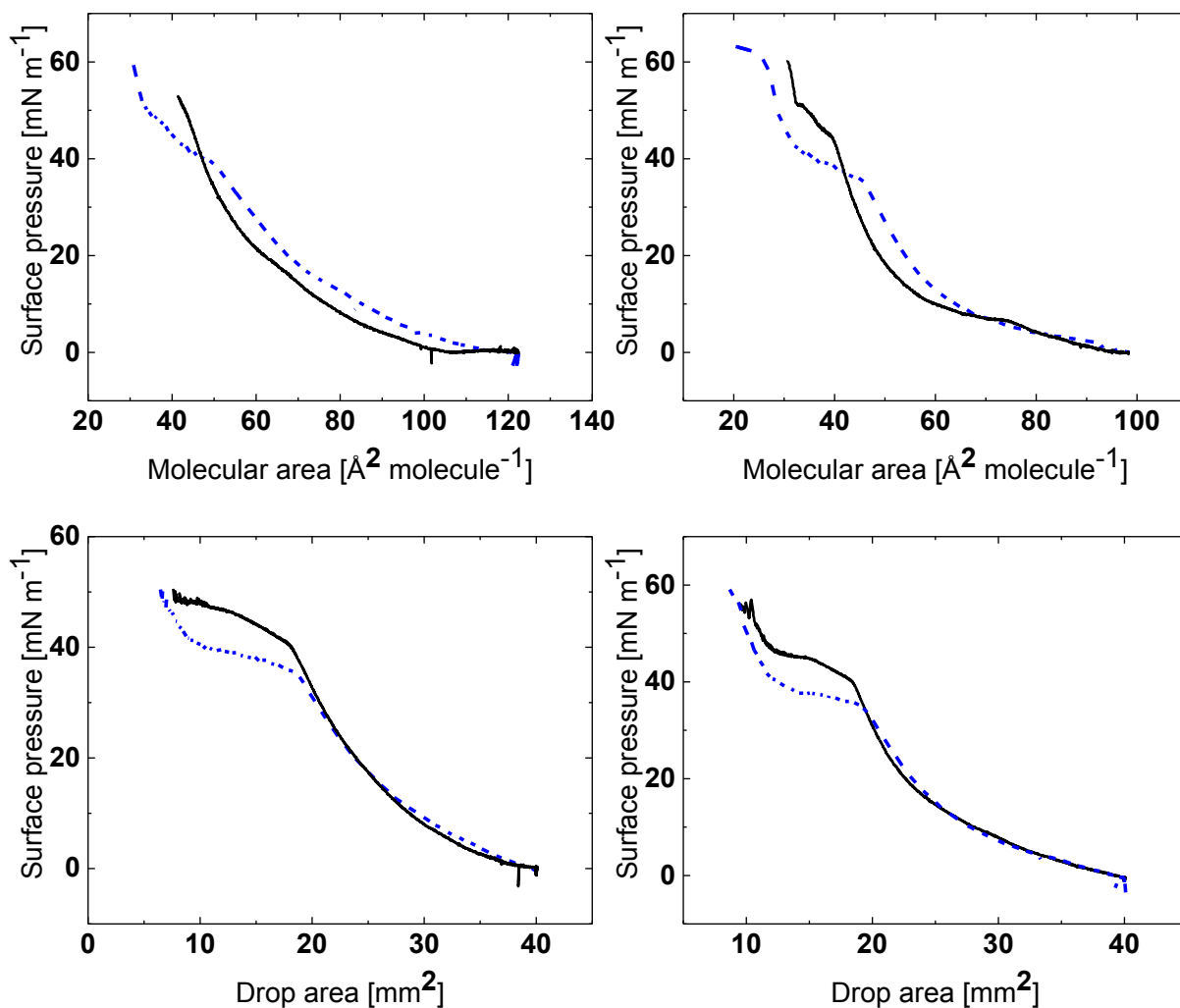
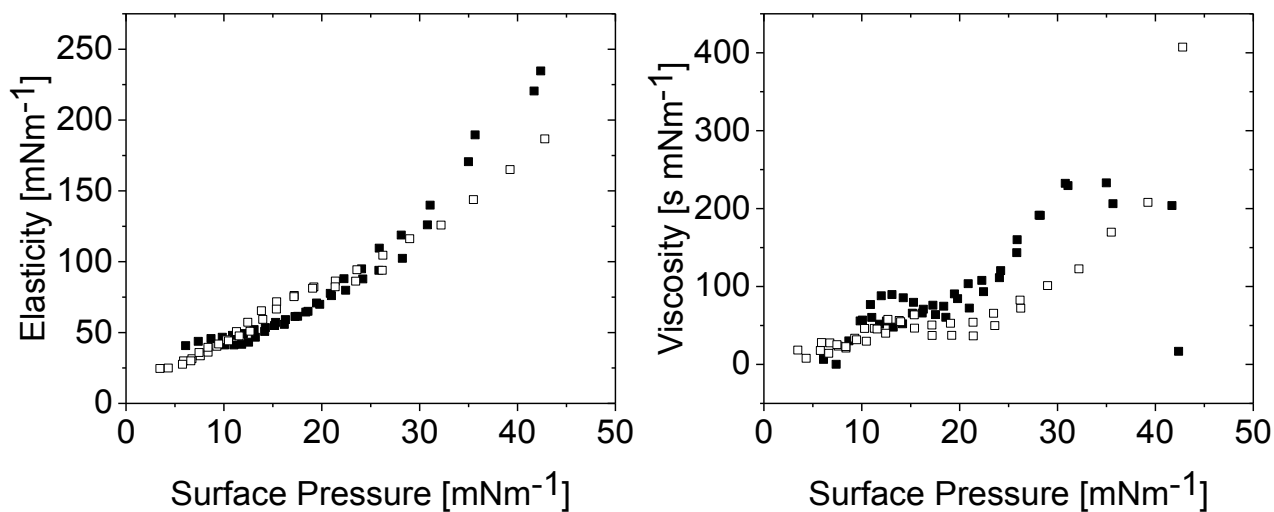
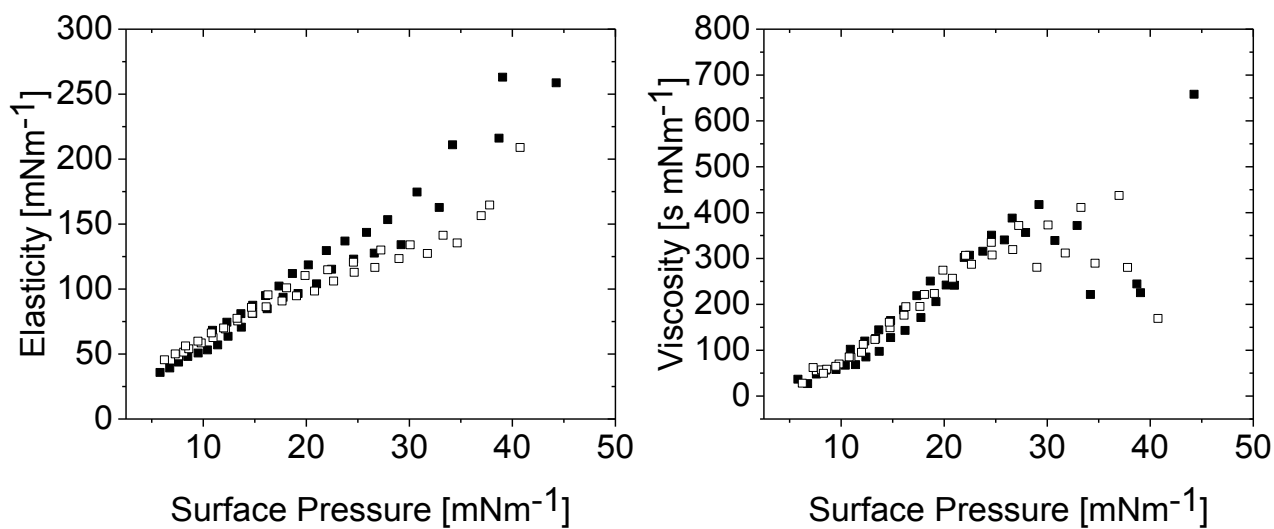


Figure A11. Isotherms of DPPC:POPG (top, left), DPPC:POPG:PA (top, right), Infasurf (bottom, left) and Survanta (bottom, right) monolayers before ozone exposure (—) and after ozone exposure (---) at 23 °C on water.



**Figure A12.** Surface dilational elasticity (left) and viscosity (right) data of DPPC:POPG before ozone exposure (■) and after ozone exposure (□) on water.



**Figure A13.** Surface dilational elasticity (left) and viscosity (right) data of DPPC:POPG:PA before ozone exposure (■) and after ozone exposure (□) on water.

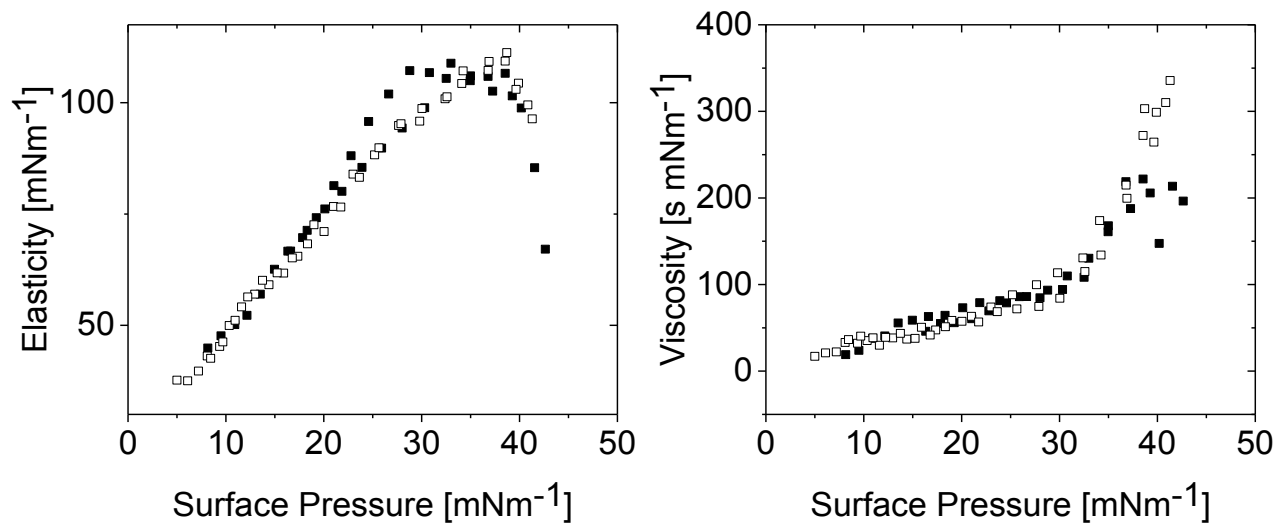


Figure A14. Surface dilational elasticity (left) and viscosity (right) data of Infasurf before ozone exposure (■) and after ozone exposure (□) on water.

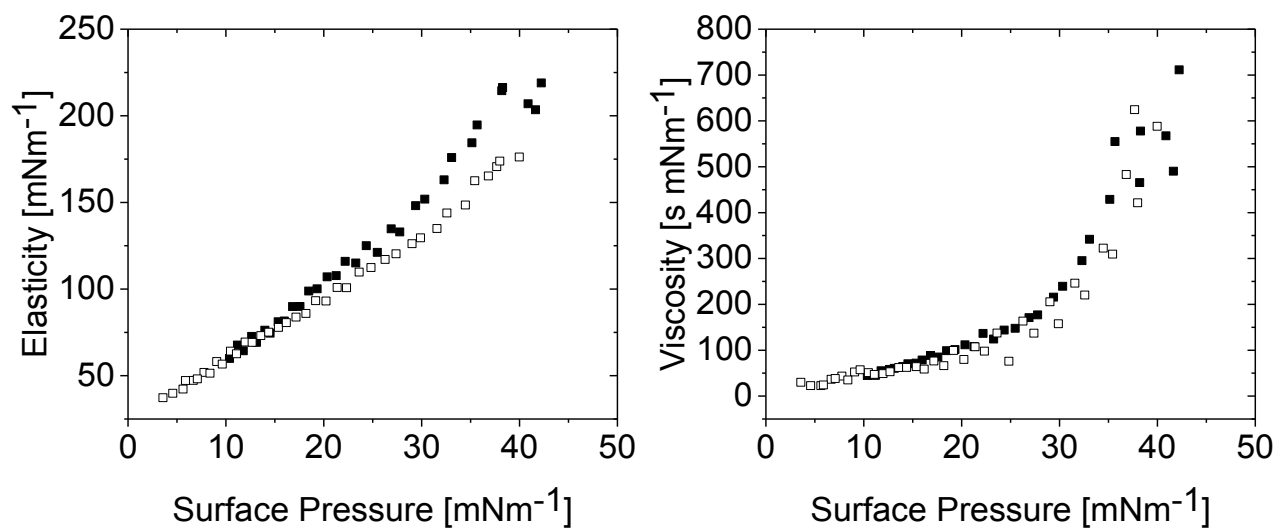
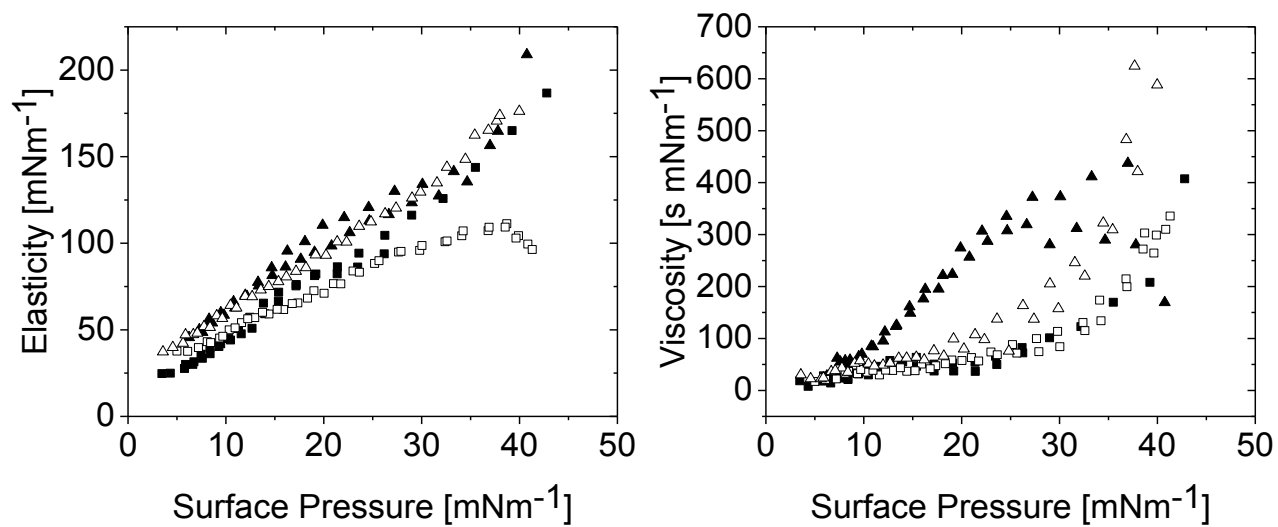


Figure A15. Surface dilational elasticity (left) and viscosity (right) data of Survanta before ozone exposure (■) and after ozone exposure (□) on water.



**Figure A16. Surface dilational elasticity and viscosity of DPPC:POPG (■), DPPC:POPG:PA (▲), Infasurf (□) and Survanta (△) on water after ozone exposure.**